Functional properties of K^+ currents in adult mouse ventricular myocytes

Judith Brouillette[1,2], Robert B. Clark[3], Wayne R. Giles[3,4] and Céline Fiset[1,2]

[1] *Research Center, Montreal Heart Institute and* [2] *Faculty of Pharmacy, University of Montreal, Montréal, Québec, Canada*
[3] *Department of Physiology and Biophysics, University of Calgary, Faculty of Medicine, Calgary, Alberta, Canada T2N 4 N1*
[4] *Department of Bioengineering, University of California, San Diego, CA, 92093-0412, USA*

Although the K^+ currents expressed in hearts of adult mice have been studied extensively, detailed information concerning their relative sizes and biophysical properties in ventricle and atrium is lacking. Here we describe and validate pharmacological and biophysical methods that can be used to isolate the three main time- and voltage-dependent outward K^+ currents which modulate action potential repolarization. A Ca^{2+}-independent transient outward K^+ current, I_{to}, can be separated from total outward current using an 'inactivating prepulse'. The rapidly activating, slowly inactivating delayed rectifier K^+ current, I_{Kur}, can be isolated using submillimolar concentrations of 4-aminopyridine (4-AP). The remaining K^+ current, I_{ss}, can be obtained by combining these two procedures: (i) inactivating I_{to} and (ii) eliminating I_{Kur} by application of low concentration of 4-AP. I_{ss} activates relatively slowly and shows very little inactivation, even during depolarizations lasting several seconds. Our findings also show that the rate of reactivation of I_{to} is more than 20-fold faster than that of I_{Kur}. These results demonstrate that the outward K^+ currents in mouse ventricles can be separated based on their distinct time and voltage dependence, and different sensitivities to 4-AP. Data obtained at both 22 and 32°C demonstrate that although the duration of the inactivating prepulse has to be adapted for the recording temperature, this approach for separation of K^+ current components is also valid at more physiological temperatures. To demonstrate that these methods also allow separation of these K^+ currents in other cell types, we have applied this same approach to myocytes from mouse atria. Molecular approaches have been used to compare the expression levels of different K^+ channels in mouse atrium and ventricle. These findings provide new insights into the functional roles of I_{Kur}, I_{to} and I_{ss} during action potential repolarization.

(Resubmitted 10 May 2004; accepted after revision 19 July 2004; first published online 22 July 2004)
Corresponding author C. Fiset: Research Center, Montreal Heart Institute, 5000 Bélanger Est, Montréal, Québec, Canada H1T 1C8. Email: celine.fiset@icm-mhi.org

The extensive efforts to develop transgenic mouse models of cardiovascular diseases have resulted in strong interest in defining the functional properties and molecular basis of the K^+ currents in mouse heart. Accordingly, a number of detailed studies focusing on K^+ currents in adult mouse ventricular myocytes have appeared (Benndorf *et al.* 1987; Wang & Duff, 1997; Barry *et al.* 1998; Babij *et al.* 1998; Zhou *et al.* 1998, 2003; London *et al.* 1998*a*,*b*; 2001; Guo *et al.* 1999, 2000; Wickenden *et al.* 1999; Xu *et al.* 1999*a*,*b*; DuBell *et al.* 2000; Jeron *et al.* 2000; Zaritsky *et al.* 2001; Kuo *et al.* 2001; Brunet *et al.* 2004; Bondarenko *et al.* 2004). In combination, these results provide a reasonably consistent and quite detailed account of the number and type of time- and voltage-dependent K^+ currents expressed in adult mouse ventricle. Although a number of different strategies have been developed for separating the total K^+ current into individual K^+ conductance components, none of these approaches are optimal for discerning the functional roles of these K^+ conductances. The separation of the outward K^+ currents in mouse ventricle is particularly challenging because a number of distinct, relatively large K^+ currents activate in a similar voltage range and with comparable kinetics. To fully understand action potential repolarization, more detailed knowledge of the biophysical properties of each of these K^+ currents is needed. In addition, understanding the functional role(s) of the different repolarizing K^+ currents

Judith Brouillette and Robert B. Clark contributed equally to this study

DOI: 10.1113/jphysiol.2004.063446

expressed in adult mouse ventricular myocytes will provide essential insights into murine models of repolarization abnormalities.

The main goals of the present study were: (1) to develop an experimental approach that allows direct determination of the amplitude and kinetics of each individual K^+ current, and yields these findings during an experimental protocol, as opposed to requiring extensive off-line analyses, (2) to provide a comprehensive description of the densities and the biophysical and pharmacological properties of the K^+ currents of adult mouse right ventricle, and (3) to use this information to determine the role of each K^+ current in modulating the repolarization phase of the action potential. In addition, we have applied these methods to adult mouse atrial myocytes. The resulting data allow a detailed comparison of the current density of the different K^+ currents which are expressed in these two heart chambers. These include: (i) a Ca^{2+}-independent transient outward K^+ current (I_{to}), (ii) an ultrarapid delayed rectifier K^+ current (I_{Kur}), and (iii) a slowly activating and non-inactivating (steady-state) outward K^+ current (I_{ss}). To relate our data to previously published molecular characterizations of K^+ channel subunits in adult mouse atria and ventricles, we have supplemented electrophysiological findings with molecular data which compare the expression levels of several K^+ channel α-subunits in the atria and ventricles of the adult mouse heart.

Methods

Isolation of myocytes

The enzymatic dispersion technique used to isolate single ventricular myocytes from adult male Swiss-Webster or CD-1 mice (2–3 months of age) has been described in detail previously (Trépanier-Boulay *et al.* 2001; Brouillette *et al.* 2003). Briefly, in accordance with the Canadian Council Animal Care guidelines, animals were heparinized, anaesthetized by inhalation of isoflurane and then killed by cervical dislocation. The hearts were rapidly removed, and retrogradely perfused through the aorta using a modified Langendorff apparatus. The following solutions were applied: (i) Hepes-buffered Tyrode solution containing (mM): 130 NaCl; 5.4 KCl; 1 $CaCl_2$; 1 $MgCl_2$; 0.33 Na_2HPO_4; 10 Hepes; 5.5 glucose (pH adjusted to 7.4 with NaOH) for 5 min; (ii) Tyrode solution without added Ca^{2+} ('Ca^{2+}-free') for 10 min; (iii) Ca^{2+}-free Tyrode solution containing 73.7 U ml^{-1} collagenase type 2 (Worthington Co. Ltd, Freehold, NJ, USA); 0.1% bovine serum albumin (BSA; Fraction V, Sigma Chemicals Co., St Louis, MO, USA); 20 mM taurine and 30 μM $CaCl_2$ for 20 min; and (iv) a 'KB' solution (Isenberg & Klockner, 1982) containing (mM): 100 potassium glutamate; 10 potassium aspartate; 25 KCl; 10 KH_2PO_4; 2 $MgSO_4$; 20 taurine; 5 creatine base; 0.5 EGTA; 5 Hepes; 0.1% BSA; 20 glucose (pH adjusted to 7.2 with KOH) for the final 5 min. During the entire perfusion procedure the solutions were maintained at 37 ± 1°C and were constantly gassed with 100% O_2. The heart was removed from the perfusion system at the end of the perfusion sequence, and the right ventricular free wall was cut into small pieces in the KB solution. The pieces were triturated gently until they were dissociated into rod-shaped single myocytes. Isolated myocytes were stored in KB solution at 4°C until use. For atrial myocytes, the methods were similar except the digestion period (iii) was 25 min. The atrial myocytes were obtained from both left and right atria.

Electrophysiological recording procedures and data analysis

An aliquot of solution containing individual myocytes was placed in a recording chamber (volume ~200 μl) mounted on the stage of an inverted microscope. After allowing 5–10 min for the myocytes to settle to the bottom of the chamber, they were continuously superfused with Hepes-buffered Tyrode solution containing (mM): 130 NaCl, 5.4 KCl, 1 $CaCl_2$, 1 $MgCl_2$, 0.33 Na_2HPO_4, 10 Hepes, and 5.5 glucose (pH adjusted to 7.4 with NaOH). 4-Aminopyridine (4-AP) was added to the Tyrode solution at the concentrations indicated. Experiments were carried out at room temperature (20–22°C), or 32 ± 1°C, as indicated. Superfusion solutions were constantly equilibrated with 100% O_2. In this study, K^+ currents were recorded in absence of L-type Ca^{2+} channels blockers, e.g. inorganic ions such as Cd^{2+}, Mn^{2+} or Co^{2+}. This allows recordings of K^+ currents and action potentials from the same myocyte and avoided the known effects of these compounds on the voltage dependence and kinetics of I_{to} (Agus *et al.* 1991). Furthermore, Ca^{2+} currents were small under the recording conditions used here (i.e. 1 mM external Ca^{2+}, room temperature), and hence the outward currents were not significantly distorted by the presence of underlying inward Ca^{2+} currents. To rule out the possibility that the K^+ currents records were significantly distorted by Ca^{2+} currents, we measured K^+ currents in the absence or presence of 100 μM cadmium chloride in the same ventricular cell. These experiments were carried out at both 22 and 32°C. At each of these temperatures, the current–voltage relations of K^+ currents recorded with and without cadmium were not significantly different, although the membrane potential dependence of I_{to} was shifted to more depolarized membrane potentials (data not shown).

Whole-cell voltage and current recordings were made using a patch-clamp amplifier (Axopatch 200B, Axon Instruments, Foster City, USA). Pipettes were made from borosilicate glass (World Precision Instruments, Sarasota, FL, USA), and had resistances in the range 1.5–4 MΩ when

filled with the following solution (mM): 110 potassium aspartate, 20 KCl, 8 NaCl, 1 $MgCl_2$, 1 $CaCl_2$, 10 EGTA or BAPTA, 4 K_2ATP and 10 Hepes (with EGTA, pCa ~8.2; with BAPTA, pCa ~7.5) (pH adjusted to 7.2 with KOH). Pipette series resistance in the whole-cell mode was in the range of 4–8 MΩ; series resistance (R_s) compensation was applied to reduce R_s by 80–90%. Voltage-clamp currents were low-pass filtered at 1 kHz with a 4-pole Bessel analog filter, digitized at 4 kHz and stored in a microcomputer using PCLAMP 8.0 software (Axon Instruments).

Voltage-clamp protocols and data analysis

Current magnitudes were normalized to cell capacitance. Capacitative currents elicited by a 10 mV depolarizing step from a holding potential of −80 mV were filtered at 10 kHz and digitized at 25 kHz. Cell capacitance was determined from the integral of these current transients. The mean capacitance of a sample of adult mouse right ventricular cells was 84.2 ± 5.6 pF ($n = 24$). The mean resting membrane potential of right ventricular myocytes was −73.7 ± 0.8 mV ($n = 42$).

Recorded membrane potentials were corrected by −10 mV to compensate for the patch pipette–bath liquid junction potential. The voltage dependence of steady-state inactivation was obtained using a two-step protocol consisting of an 'inactivating pre-pulse' to selected potentials (between −110 and −20 mV), followed by a fixed 'test' pulse to +30 mV. The duration of the inactivating and test pulses depended on which current component was being measured; details are given in Results. The test current amplitude at each prepulse potential was normalized to the maximal amplitude of this current (I/I_{max}), and plotted as a function of the inactivating prepulse potential. Data were fitted to a Boltzmann equation:

$$I/I_{max} = 1/[1 + \exp((V_m - V_{1/2})/S_{1/2})]$$

where $V_{1/2}$ represents the membrane potential (V_m) at which 50% of the channels are inactivated and $S_{1/2}$ is the mid-point slope factor. Recovery from inactivation was studied using a two-step protocol in which an inactivating step to +30 mV was followed by an identical test step, delivered at a series of time intervals between the inactivating and test steps. The ratio of the current amplitude elicited by the second (test) to the first (inactivating) pulse (P_2/P_1) was plotted as a function of the interpulse interval yielding the time course of recovery from inactivation. Exponential functions were fitted to these data as described below.

Current sizes were measured relative to the zero current level, except where noted. Plotting of membrane voltage and current records, and curve fitting of Boltzmann equation and exponential functions were done using SIGMAPLOT (Jandel Scientific Software, CA, USA), Origin (OriginLab, MA, USA) and Clampfit (Axon Instruments).

Ribonuclease protection assay

An RNase protection assay was used to compare the mRNA levels for Kv1.5, Kv2.1, Kv4.2 and Kv4.3 K^+ channel α-subunits in ventricular and atrial tissues obtained from adult male mice. The preparation of the RNA and the RNase protection assay were performed as previously described (Trépanier-Boulay *et al.* 2001). For ventricular RNA, only the lower (apical) 3/4 of the ventricles was used to ensure that no atrial or aortic tissue was present. For atrial RNA, only left and right atrial appendages were used. Areas around the major vessels were removed to avoid inclusion of vascular tissue and/or parasympathetic cardiac ganglia. The wet weights were about 100 mg for ventricular tissue, and 5 mg for atrial tissue. Each atrial sample used for RNA extraction was pooled from dissections of four or five animals. Transcription was carried out using the MAXIscript In Vitro transcription kit (Ambion; Austin, TX, USA). The RNase protection assays were performed using the RPA III Kit (Ambion). The total RNA samples and the probes were hybridized at 48°C overnight. Mouse β-actin was included in all reactions as an internal control. The mRNA transcript levels were quantified on a Bio-Rad PhosphoroImager.

Statistical analysis

Averaged values are shown as mean ± S.E.M., and n refers to the number of different cells. Parameters obtained from curve fitting are shown as the value ± S.E.M. Statistically significant differences ($P < 0.05$) were determined with a two-tailed, paired or unpaired Student's t test, or an analysis of variance, when appropriate.

Results

Separation of the three outward K^+ currents in mouse ventricle: I_{to}, I_{Kur}, I_{ss}

The complex and multiphasic decay of outward currents in adult mouse ventricular myocytes reflects the differential inactivation of the K^+ currents which are expressed in this tissue (Xu *et al.* 1999*b*). It is known that the inactivation of each of these K^+ currents exhibits distinct time and voltage dependence. Advantage can be taken of the presence of 'fast' and 'slow' phases of inactivation of these currents in specifying voltage-clamp 'inactivating' protocols to emphasize or isolate the different K^+ conductances. In our study, based in part on previous results, which demonstrated that the inactivation phase of K^+ currents in mouse ventricle is multiexponential, a voltage protocol was designed to selectively inactivate one component without significantly affecting the others. Figure 1*A* shows

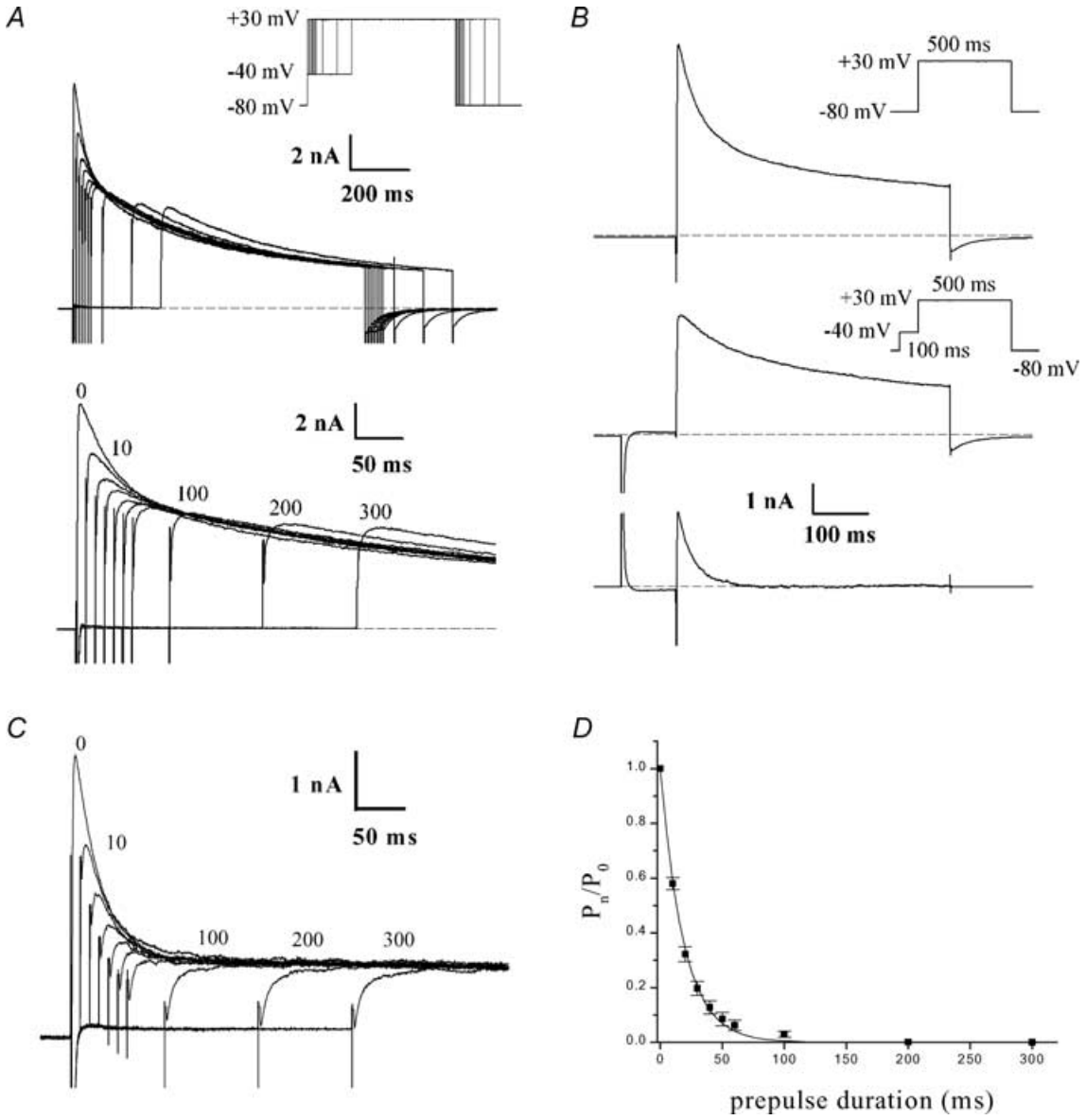

Figure 1. Isolation of rapidly inactivating component of K^+ current, I_{to}
A, effect of an 'inactivating prepulse' on outward K^+ current of a voltage-clamped adult mouse ventricular myocyte. Upper records, the voltage-clamp protocol is shown at upper right: the duration of the inactivating prepulse (−40 mV) was varied between 0 and 300 ms (0, 10, 20, 30, 40, 50, 60, 100, 200, 300 ms). Each prepulse was followed by a 500 ms step to +30 mV. Note the rapid decrease in the peak current which exhibits a fast phase of decay with progressively increasing prepulse durations. Lower records, same current records as above, on expanded time scale. Numbers next to selected current records indicate duration of prepulse. Note that fast phase of current decay was abolished by prepulses longer than about 60 ms; increasing prepulse duration further resulted in very little additional reduction in peak current. *B*, 'fast' and 'slow' phases of decaying of outward K^+ current can be separated using inactivating prepulse voltage-clamp protocol. Upper records, membrane current produced by 500 ms voltage-clamp step to +30 mV, from HP −80 mV. Middle records, the same voltage-clamp step as above was repeated, but in this case it was preceded by a 100 ms 'inactivating' prepulse to −40 mV. Note that the initial rapid phase of current decay was abolished. Lower records, difference current obtained by subtracting record with the inactivating prepulse voltage-clamp protocol from that without the prepulse. *C*, time course of inactivation of I_{to}, for prepulse of −40 mV at room temperature.The voltage protocol illustrated in *A* was repeated in the presence of 100 μM of 4-aminopyridine (4-AP). *D*, plot of the ratio of the 'difference current' at prepulse duration $t = n$ (P_n) and $t = 0$ (P_0, P_n/P_0) against prepulse duration. Data points denote mean ± S.E.M. Smooth curve is the best-fit single exponential function. Note that the data presented in Figs 1–3 were obtained at room temperature.

the effect of increasing the duration of an 'inactivating prepulse' on the most rapidly decaying component of outward current when recording at room temperature. Note that the peak outward current decreased significantly as the prepulse duration was increased from 10 ms to about 50 ms, and that it decreased further, but by a proportionally smaller amount, as the prepulse duration was further increased up to 300 ms (see below). Figure 1*B* shows that the 'fast' and 'slow' phases of inactivation of the outward current produced by a strong depolarizing step (e.g. +30 mV) can be separated using a voltage-clamp protocol which includes a short prepulse which immediately precedes the main depolarizing step. In this experiment, a 500 ms depolarizing voltage-clamp step to +30 mV produced a rapidly activating current that decayed in distinct 'fast' and 'slow' phases. If a 100 ms 'inactivating prepulse' to −40 mV preceded the +30 mV step, the initial 'fast' phase of current decay (which corresponds to I_{to}) was abolished, but there was no significant effect on the magnitude or time course of the 'slow' phase of decay. This finding was confirmed on six different myocytes. This 'voltage-sensitive' component of the current, determined by subtracting the current record obtained with the inactivating prepulse voltage-clamp protocol from the current record obtained without the prepulse, consisted of a very rapidly activating (< 2 ms) outward current that inactivated almost completely within 150–200 ms. Such voltage-sensitive difference currents obtained with longer prepulse durations (> 100 ms) often had a second, considerably slower phase of current decay which had a much smaller amplitude than the rapid one. The time course of inactivation of the voltage-sensitive current was well fitted by a single exponential function; the time constant of inactivation (at a membrane potential of +30 mV) ranged from 20 to 35 ms in 12 different myocytes (28.0 ± 1.2 ms). This voltage-sensitive difference current corresponds to the Ca^{2+}-independent transient outward current, I_{to}. Figure 1*C* shows current recordings obtained with the protocol used in Fig. 1*A* in the presence of 100 μM 4-AP. At this concentration, 4-AP blocks I_{Kur} without any significant effect on I_{to} (see below, Fig. 2). The duration of the inactivating step (−40 mV) was increased in 10 ms increments from 0 to 60 ms, and then in 100 ms increments to 300 ms. Note the decrease in peak current with increasing prepulse duration. To analyse these data, the current activated following the longest prepulse was subtracted from each of the other currents; the resulting 'difference currents' were normalized to the one obtained without prepulse. This ratio was then plotted against the inactivating prepulse duration (Fig. 1*D*). A single exponential function was fitted to the data and yielded a time constant of 19.0 ± 1.7 ms ($n = 8$). This procedure illustrates that to ensure complete inactivation of I_{to}, the duration of the inactivating prepulse should correspond to approximately 5 times its inactivation time constant (in this case 100 ms prepulse duration). The next step was to verify that the selected prepulse duration did not alter I_{Kur} (see Fig. 2).

A low concentration of 4-aminopyridine was used to block a rapidly activating, slowly inactivating outward K^+ current (I_{Kur}). The current remaining after inactivation of I_{to} is denoted I_{Kslow} and is composed of I_{Kur} (or the 4-AP-sensitive component) and I_{ss} (or the 4-AP-resistant component). Our previous work (Fiset *et al.* 1997*a*; Trépanier-Boulay *et al.* 2001; Brouillette *et al.* 2003) demonstrated that adult mouse ventricular myocytes express a K^+ current that can be blocked by low concentrations (10–200 μM) of 4-AP, results which have been confirmed by others (Zhou *et al.* 1998; Xu *et al.* 1999*b*; DuBell *et al.* 2000; London *et al.* 2001). Figure 2*A* shows the effect of 100 μM 4-AP on membrane current produced by a 500 ms voltage-clamp step, in this case to +10 mV. The main effect of 4-AP was to abolish the large, slowly inactivating phase of the current (corresponding to I_{Kur}). In the presence of 4-AP, the outward current waveform consisted of a transient current that rapidly decayed to a constant level by the end of the 500 ms voltage-clamp step. Figure 2*A* also compares the effect of an inactivating prepulse on the membrane currents before and after the addition of 4-AP. As shown in Fig. 1, in the absence of 4-AP the prepulse abolished the rapidly inactivating component of the current (I_{to}). The prepulse had a very similar effect in the presence of 4-AP: the initial transient current component (I_{to}) was abolished by the prepulse, leaving a current that slowly activated to a constant magnitude during the duration of the voltage-clamp step (I_{ss}; see below). The magnitude and time course of the 4-AP-sensitive current was obtained by subtracting current records after application of 4-AP from those obtained in the absence of 4-AP. Since two different voltage-clamp protocols were used (i.e. a depolarizing step with or without the inactivating prepulse), the 4-AP-sensitive current (or I_{Kur}) could be obtained by subtracting two different pairs of current records. Figure 2*A* shows that the 4-AP-sensitive currents obtained by subtracting pairs of currents (i.e. before and after 4-AP), obtained either with or without the inactivating prepulse, were virtually identical in magnitude and time course, demonstrating that the inactivating prepulse had no significant effect on the 4-AP-sensitive current. Very similar results were obtained when these subtraction experiments were repeated on six different cells. This is shown in Fig. 2*C*. The 4-AP-sensitive current activated rapidly, but inactivated much more slowly than I_{to}. By the end of the 500 ms voltage-clamp steps to +10 mV, this current had inactivated to about 30% of its peak. Complete inactivation of the 4-AP-sensitive current required voltage-clamp steps of at least 2 s duration (cf. Fig. 3). Figure 2*A* shows that the rapidly activating, slowly

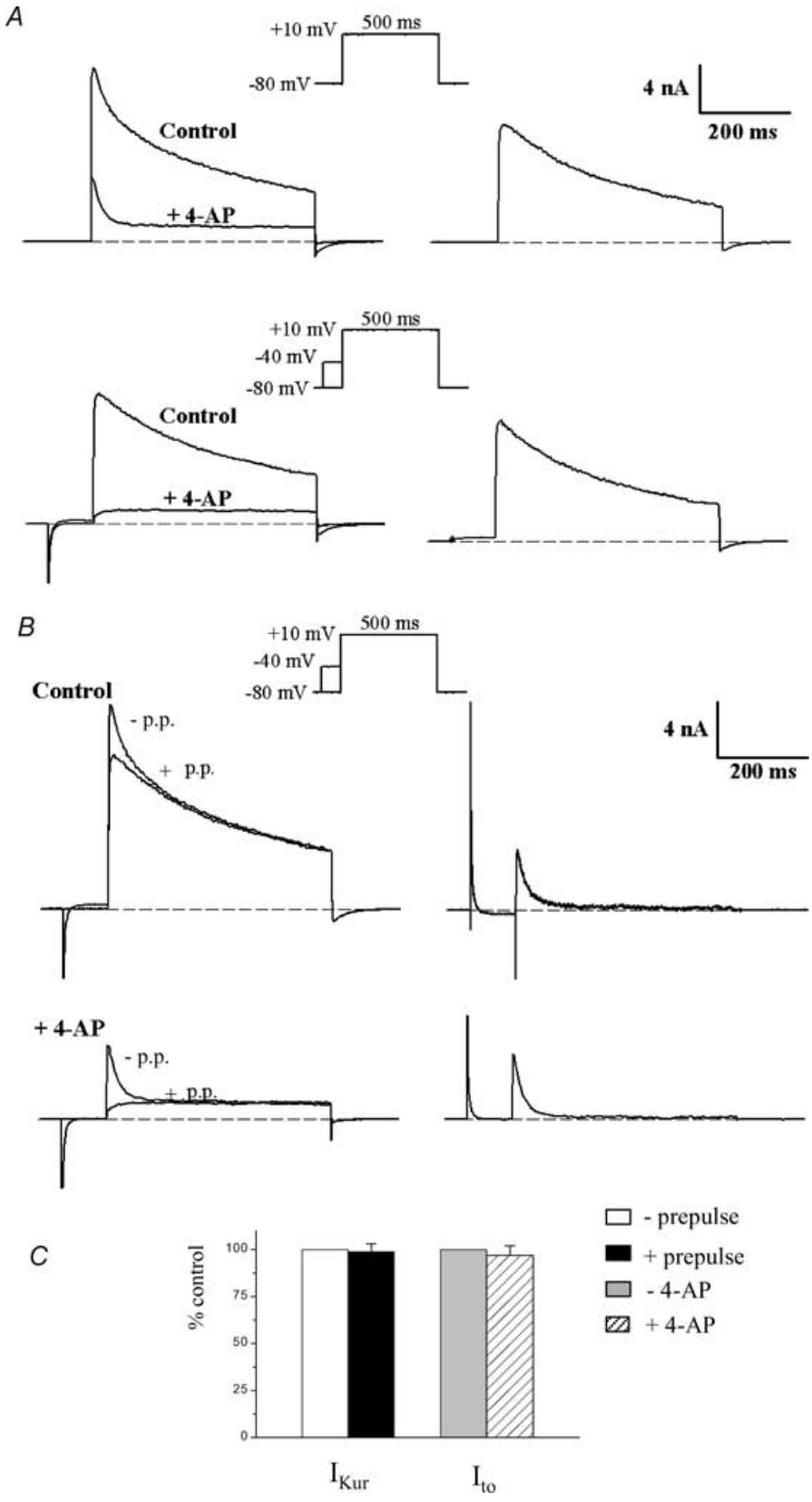

Figure 2. Low concentration of 4-aminopyridine (4-AP) selectively blocks the rapidly activating, slowly inactivating outward current, I_{Kur}
Left column in *A*, superimposed pairs of current records, before ('control') and after application of 100 μM 4-AP ('+4-AP'). The upper pair of currents was produced by a 500 ms step to +10 mV (HP −80 mV). The lower pair of records was produced by an identical step which was preceded by an inactivating prepulse (100 ms, −40 mV). Right column in *A*, 4-AP-sensitive 'difference' currents, obtained by subtraction (control −4-AP), for each pair of records at left. Note that the difference current was the same whether or not the depolarizing step was preceded by the inactivating prepulse. Left column in *B*, the current records in *A* were rearranged, so that both control records are superimposed, and both '+4-AP' records are superimposed. Right column in *B*, potential-sensitive 'difference' currents, obtained by subtraction of currents obtained with and without the inactivating prepulse. Note that the difference current, I_{to}, was very similar in the presence and in the absence of 4-AP. *C*, bars graph comparing I_{Kur} and I_{to} amplitude recorded at +10 mV with and without prepulse or 4-AP, respectively ($n = 6$). I_{Kur} and I_{to} recorded in absence of prepulse or 4-AP were set to 100%. Comparable results were also obtained for test pulses of +30 mV (data not shown).

inactivating outward K^+ current (I_{Kur}) can be isolated (identified) using a low concentration of 4-AP and that this current is not affected by the prepulse used to inactivate I_{to}. Additional experiments using a different depolarizing voltage (+ 30 mV instead of +10 mV) showed that the subtraction procedure yielded similar results (e.g. Fig. 12).

To evaluate the selectivity of this pharmacological manoeuvre additional experiments were done to evaluate whether the concentration of 4-AP used to block I_{Kur} altered I_{to}. Figure 2*B* shows that I_{to} obtained by subtracting the pairs of currents (with and without the prepulse) in control conditions was very similar to I_{to} obtained by subtracting the pairs of currents in the presence of 4-AP. Similar results were obtained in six different cells (see Fig. 2*C*). Comparable results were also obtained for test pulses of +30 mV (data not shown). These data are consistent with the relatively low sensitivity of I_{to} in mammalian myocytes to 4-AP; the 50% blocking concentration of 4-AP is in the range 1–5 mM (Josephson *et al.* 1984; Wettwer *et al.* 1993; Campbell *et al.* 1995; Fiset *et al.* 1997*b*), hence 100 μM 4-AP would be expected to have little effect on the amplitude of I_{to}.

The third component of outward K^+ current in adult mouse ventricle is a slowly activating, 4-AP-resistant current (I_{ss}). The '4-AP-resistant' outward current that remained in the presence of 100 μM 4-AP (Fig. 2) resembled a relatively slowly activating, non-inactivating delayed rectifier. However, block of K^+ channels by 4-AP can exhibit complex time and voltage dependence (Campbell *et al.* 1995; Tseng *et al.* 1996). It was therefore very important to establish whether the residual 4-AP-resistant current was a component distinct from I_{to} and I_{Kur}, or whether it resulted from incomplete block by 4-AP of I_{Kur}. Figure 3 shows data from an experiment that was designed to distinguish between these possibilities. In this experiment, a depolarizing voltage-clamp step that was of sufficient duration (in this case, 5 s) to completely inactivate I_{Kur} was applied to a ventricular myocyte. This long depolarizing step was followed by a second, shorter (750 ms) depolarizing step. A brief (100 ms) 'gap', at −40 mV, was interposed between the two depolarizing steps. Note that in control conditions the current produced by the second depolarizing step activated slowly, and maintained a constant amplitude throughout the 750 ms

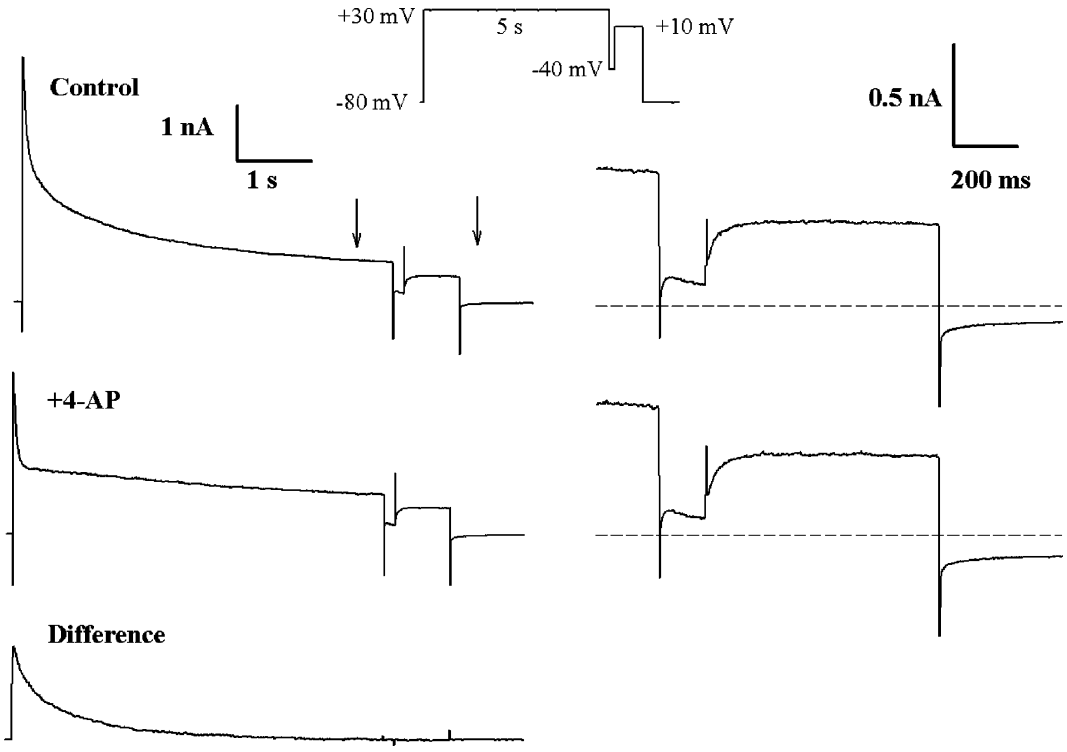

Figure 3. Inactivation of I_{Kur} reveals a third component of outward current, I_{ss}
Left column, membrane currents produced by a double-pulse voltage-clamp protocol (inset), consisting of a 5 s, +30 mV step, and a 0.75 s, +10 mV step. The depolarizing steps were separated by a 100 ms 'gap' at −40 mV. The 'difference' current (I_{Kur}) was obtained by subtracting the control current, and the current after application of 100 μM 4-AP (+4-AP). Note that I_{Kur} was completely inactivated by the end of the 5 s step. The time and current calibrations are identical for all three current traces. Right column, the membrane currents produced by the step to +10 mV are shown on expanded time and current scales (see vertical arrows at left). The dashed lines indicate zero current. This current was slowly activating, and showed no significant inactivation during the 0.75 s step. Note that the currents are identical in the presence and absence of 100 μM 4-AP.

step. The same voltage-clamp protocol was repeated after application of 100 μM of 4-AP. As shown in Fig. 2, the slowly inactivating component of current elicited by the first depolarizing step was abolished by 4-AP; however, the slowly activating current produced by the second depolarizing step was identical to that recorded under control conditions. Subtraction of the current records before and after application of 4-AP showed that the 4-AP-sensitive current (i.e. I_{Kur}), which was activated by the first step was completely inactivated by the end of the 5 s step. Subtraction of these currents also showed that there was no net difference current during the second step; this finding indicates that the current activated in the absence of I_{Kur} was very similar whether I_{Kur} was removed by either inactivation, or by block by 4-AP. These data confirm that the 4-AP-resistant current is a K^+ current which is distinctly different from either I_{to} or I_{Kur}, and that its slow activation kinetics are not an artefact due to complex channel blocking actions of 4-AP. These results also demonstrate that the concentration of 4-AP used to block I_{Kur} did not affect the non-inactivating current since the amplitude of the currents elicited by the second pulse in the absence or presence of 4-AP were identical. This 4-AP-resistant delayed rectifier showed little inactivation, even during long depolarizations (Fig. 3); accordingly, it is denoted as the 'steady-state' current, or 'I_{ss}'.

Separation of the outward K^+ current at 32°C

Figures 1–3 describe the strategy used to separate the outward K^+ currents which are expressed in adult mouse ventricular myocytes when recorded at room

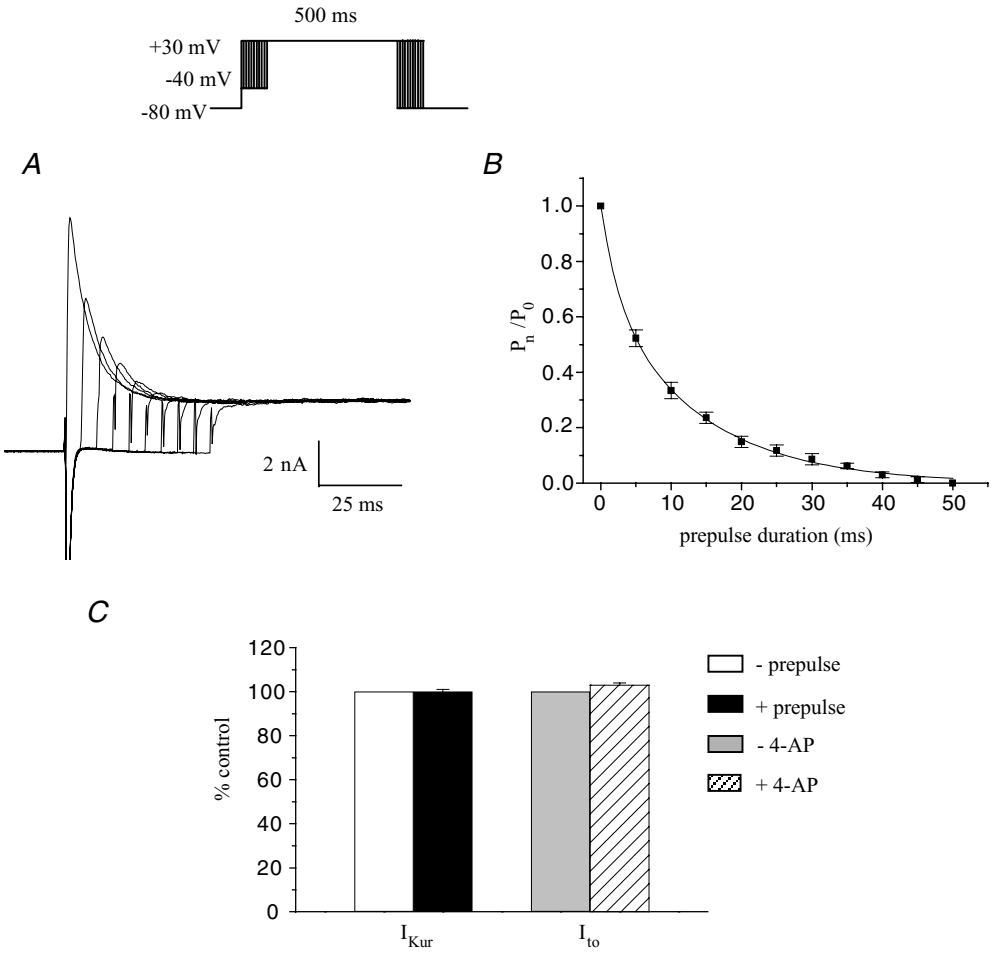

Figure 4. Time course of inactivation of I_{to}, for prepulse of −40 mV at 32°C
A, current traces obtained with a 500 ms step to +30 mV preceded by a −40 mV inactivating prepulse of various durations (0, 5, 10, 15, 20, 25, 30, 35, 40, 45 ms) are shown. Currents were recorded in the presence of 100 μM 4-AP. *B*, plot of the ratio of the 'difference currents' against prepulse duration. The current following the 50 ms prepulse was subtracted from each current to obtain a 'difference current' (P_n) at every prepulse duration. These difference currents were then normalized to the difference current obtained without prepulse (P_0, P_n/P_0). Smooth curve is the best-fit single exponential function. *C*, bar graph comparing I_{Kur} and I_{to} amplitude recorded at +10 mV with and without prepulse or 4-AP, respectively ($n = 5$, differences not significant). I_{Kur} and I_{to} recorded in absence of prepulse or 4-AP were set to 100%. Comparable results were also obtained for test pulses of +30 mV (data not shown).

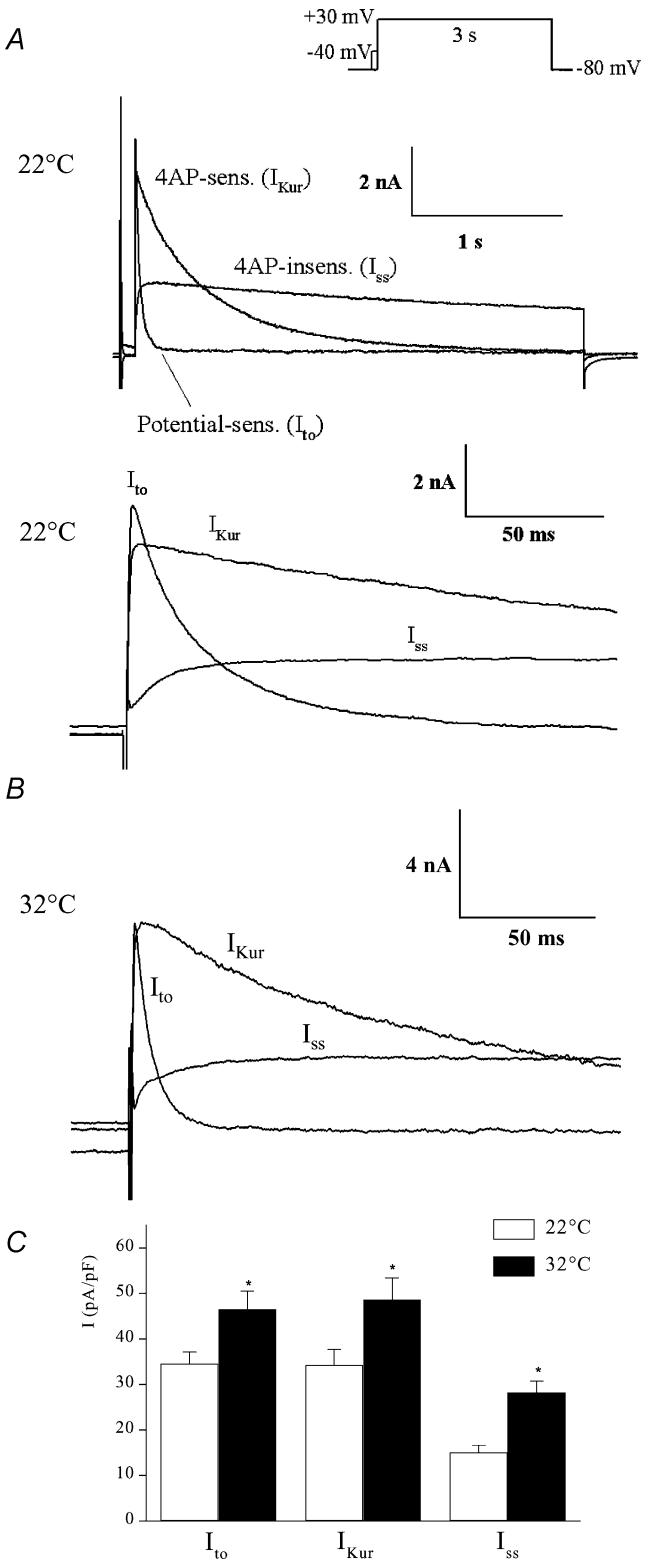

Figure 5. Comparison of magnitude and kinetics of I_{to}, I_{Kur} and I_{ss} in adult mouse ventricular myocytes recorded at 22 and 32°C
Upper records in *A*, superimposed potential-sensitive (I_{to}), 4-AP-sensitive (I_{Kur}) and 4-AP-insensitive (I_{ss}) current components, separated using 100 μM 4-AP and inactivating prepulse voltage-clamp protocols, as described in Figs 1 and 2. The voltage-clamp step was +30 mV, for 3 s (upper right). Note the very large difference in rate of inactivation of these three currents. Lower records in *A*, the same set of records is shown on a much faster time scale. Note that I_{to} and I_{Kur} activate very quickly compared with I_{ss}. *B*, repetition of the protocol shown in *A* with the exception that the currents were recorded at 32°C. Note the expanded time scale. *C*, bar graph represents mean (± S.E.M.) peak current density of each of the three components of outward K^+ current recorded at 22 or 32°C, measured at a test potential of +30 mV from a HP of −80 mV. The data obtained at 22 and 32°C were averaged from 12 and 10 different ventricular myocytes, respectively. $^*P < 0.05$.

temperature. To determine whether this method is also valid when data are obtained at more physiological temperatures, we repeated the experiments presented in Fig. 1*C* at 32°C. Our results demonstrate that although the protocol has to be adapted, the same strategy can be applied at more physiological temperatures. At 32°C, a 100 ms prepulse completely inactivated I_{to} but also inactivated a fraction of I_{Kur} due to its faster kinetics at warmer temperatures (data not shown). Accordingly, the duration of the inactivating prepulse had to be reduced. To establish the appropriate parameters for the separation protocol to be used at 32°C, we applied the same strategy that we used at room temperature (see Figs 1 and 2). Figure 4 presents data obtained at 32°C with the protocol outlined in Fig. 1 in the presence of 100 μM 4-AP. The duration of the inactivating prepulse varied from 5 to 50 ms. At 32°C, the peak current was decreased following a much shorter prepulse than at room temperature because the time constant of inactivation of I_{to} (calculated from the plot of the ratio of the 'difference currents' (P_n/P_0) *versus* the prepulse duration) was significantly faster at 32°C; the time constant of I_{to} inactivation was 10.1 ± 0.7 ms at 32°C, and at 22°C it was 19.0 ± 1.7 ms. These data were obtained from seven different cells and are presented in Fig. 4*B*. Based on these results, the duration of the inactivating prepulse at 32°C was set to 50 ms. We repeated the experiments presented in Fig. 2 at 32°C and confirmed that a 50 ms prepulse had no detectable effect on I_{Kur} and also showed that the effect of 100 μM 4-AP on I_{to} at 32°C was minimal (Fig. 4*C*). This pattern of results was observed in each of the six different myocytes studied.

Contribution of current components to *I–V* relationship and ventricular action potential

The data shown in Figs 1–4 and results from other laboratories (Heath *et al.* 1998; Zhou *et al.* 1998; Xu *et al.* 1999*b*; DuBell *et al.* 2000; Knollmann *et al.* 2000; Nerbonne, 2000; Brunet *et al.* 2004) make it clear that outward K^+ currents in adult mouse right ventricular myocytes consist of at least three distinct components. Each has different kinetics of activation and inactivation, a distinct voltage range for inactivation, and sensitivity to block by 4-AP. To gain information concerning the functional significance of these currents, it is

necessary to determine their relative magnitudes, and hence their contributions to the peak *I–V* relationship. Figure 5*A* illustrates an example of the three K^+ current components activated in a ventricular myocyte by a voltage-clamp step to +30 mV and recorded at room temperature.

The components of K^+ current were isolated using the voltage-clamp and pharmacological protocols outlined in Figs 1 and 2. Figure 5*B* shows an example of the three outward K^+ currents activated at 32°C by a +30 mV step. As expected, the kinetics of activation and inactivation of each current component were faster and the amplitude was larger at 32°C than at room temperature. Note however, that at both 22 and 32°C, I_{to} and I_{Kur} were the two largest components. This pattern of responses was observed in the majority (> 95%) of the right ventricular myocytes studied. The mean peak current densities (at +30 mV) of each of the three components recorded at 22°C and 32°C are shown in Fig. 5*C*. The current densities of I_{Kur} and I_{to} were not significantly different from each other, while I_{ss} was significantly smaller than either I_{Kur} or I_{to} ($P < 0.05$) at both temperatures. The activation threshold for I_{Kur} and I_{to} was about −40 mV; I_{ss} was first detectable at about −30 mV. All three current components exhibited outward rectification over the potential range of −40 to +50 mV.

Visual inspection of the recording presented in the lower panel of Fig. 5*A* shows that the activation rate differed significantly amongst these three K^+ currents. We measured the rate of activation by fitting the activation phase of each type of K^+ current with a single exponential function. Figure 6 presents the activation time constants for the three K^+ currents. These parameters were obtained at two different membrane potentials (+10 and +30 mV) at room temperature. At both membrane potentials, both I_{to} and I_{Kur} had fast activation rates while I_{ss} activated much more slowly. For example, at +10 mV, the activation rate of I_{ss} was 30 times and 11 times slower than that of I_{to} and I_{Kur}, respectively. All three K^+ currents displayed a faster activation at +30 mV compared to +10 mV, but this difference was more pronounced for I_{ss}.

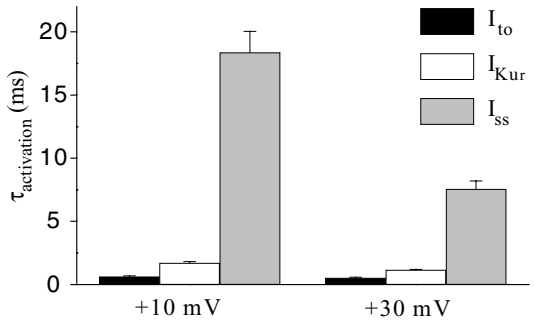

Figure 6. Comparison of activation kinetics of I_{to}, I_{Kur} and I_{ss} in adult mouse ventricular myocytes at room temperature (22°C)
Bar graph showing mean (± S.E.M.) activation time constants for I_{to}, I_{Kur} and I_{ss} recorded at two different voltages, +10 and +30 mV, from 12 ventricular myocytes at room temperature. Each current exhibited distinct activation kinetics.

Mouse ventricular myocytes have action potentials that are very brief compared with most other mammalian cardiac action potentials (Fiset *et al.* 1997*a*; Barry *et al.* 1998; London *et al.* 1998*a*, 2001; Trépanier-Boulay *et al.* 2001; Knollmann *et al.* 2001; Danik *et al.* 2002; Brouillette *et al.* 2003; Brunet *et al.* 2004). We previously reported that action potentials in isolated adult mouse ventricular cells (4 Hz, room temperature) had 50 and 90% duration, which averaged 6.0 and 20.7 ms (Fiset *et al.* 1997*a*), respectively, and that action potential duration (APD) was significantly prolonged by concentrations of 4-AP that selectively blocked I_{Kur} (Fiset *et al.* 1997*a*; Trépanier-Boulay *et al.* 2001). Figure 7*A* and *C* shows an example of the effect of blocking I_{Kur} on the action potential waveform, and on the K^+ currents activated at membrane potentials near the peak of the action potential, recorded from the same ventricular myocyte at room temperature. In control conditions, the peak of the action potential was about +40 mV, and complete repolarization occurred within about 25 ms. In the presence of 100 μM of 4-AP, neither the resting membrane potential nor the peak overshoot of the action potential were changed, but the time course of repolarization was prolonged dramatically. For the example shown in Fig. 7*A*, the 90% repolarization time increased from 13.7 ms to 49.5 ms. The maximum rate of repolarization of the action potential (Fig. 7*B*), which occurred less than 1 ms after the peak, was reduced from −48.6 to −23.1 V s^{-1} by 100 μM 4-AP. In seven myocytes, the maximum rate of repolarization was reduced from -39.0 ± 2.5 to -17.3 ± 2.3 V s^{-1} after application of 100 μM 4-AP ($P < 0.001$; paired *t* test). In addition, the membrane potential at which the maximum rate of repolarization occurred was more depolarized after application of 4-AP than it was in control conditions. For the example shown in Fig. 7*A*, the maximum rate of repolarization occurred at +17.2 mV in control conditions, and +27.2 mV after 4-AP; for the same seven myocytes, the maximum rate of repolarization occurred at $+13.9 \pm 3.8$ mV before and $+23.7 \pm 3$ mV after application of 4-AP ($P < 0.01$; paired *t* test). Figure 7*C* shows the net membrane currents produced by a voltage-clamp step from the resting membrane potential to the peak of the action potential. In control conditions, the peak outward current was 14.5 nA at this membrane potential (+40 mV); the peak current was reduced to 7.1 nA after blocking I_{Kur} with 100 μM 4-AP. This large reduction in the magnitude of outward current contributed significantly to the more than 2-fold increase in action potential duration measured at 90% of repolarization. The experiment illustrated in Fig. 7*A* was repeated with a different myocyte at 32°C. For the example presented in Fig. 7*D*, the 90% repolarization time increased from 20.3 to 49.4 ms in the presence of 100 μM

4-AP. Figure 7*E* shows mean action potential durations measured at 20, 50 and 90% of repolarization recorded at 22 and 32°C in the absence or in the presence of 100 μM 4-AP. Under control conditions (without 4-AP) APD_{20} and APD_{50} were significantly shorter at 32°C than at room temperature, while APD_{90} was not significantly different at both temperatures. The block of I_{Kur} by 100 μM 4-AP produced a comparable prolongation of the APD at 22 and 32°C, suggesting that the contribution of this current to the action potential waveform was similar at both temperatures.

Inactivation/reactivation of I_{to} in adult mouse ventricular myocytes

Figure 8 shows the membrane potential dependence of 'steady-state' inactivation for I_{to}, obtained with a two-pulse protocol at 22°C (see Methods). The 100 ms

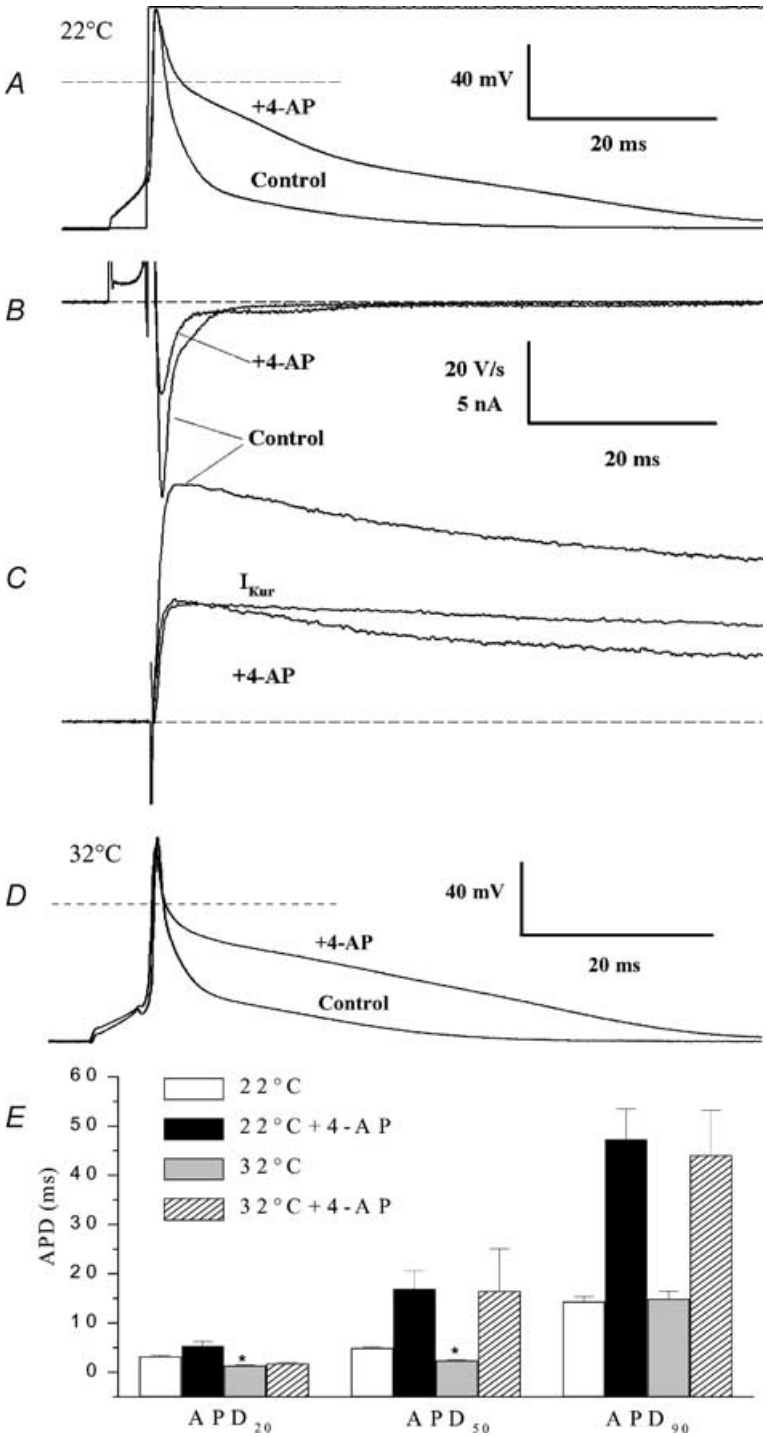

Figure 7. Role of I_{Kur} in repolarization of adult mouse ventricular action potential
A, comparison of action potentials recorded at room temperature before (control) and after application of 100 μM of 4-AP (+4-AP) in the same myocyte. Stimulation frequency was 1 Hz. Voltage-clamp step to +40 mV is also shown. Dashed line indicates zero membrane potential. *B*, first derivative (d*V*/d*t*) of action potentials before and after 100 μM AP. *C*, membrane currents produced by a depolarizing step to +40 mV from a HP of −80 mV in same myocyte, before and after application of 100 μM of 4-AP. I_{Kur} ('4-AP-sensitive' current) was obtained by subtraction. The voltage-clamp step (and hence the current) was aligned to coincide with the end of the waveform stimulus current. Dashed line indicates zero current. *D*, comparison of action potentials recorded at 32°C before (control) and after application of 100 μM 4-AP (+4-AP) in the same myocyte. Stimulation frequency was 1 Hz. *E*, bar graph showing mean (± S.E.M.) duration of actions potentials recorded without and with 4-AP at 22°C (open and black bars, $n = 10$ for both groups) and at 32°C (grey and hatched bars, $n = 9$ and 5, respectively). *$P < 0.05$ *versus* 22°C without 4-AP group.

inactivating prepulse was varied from −110 to −20 mV in 10 mV increments. The currents recorded with inactivating prepulses was of −30 or −20 mV were not identical to that recorded with the −40 mV prepulse. There was an additional reduction of peak current at these voltages, compared with the −40 mV prepulse (see Fig. 8*A*). We attempted to determine whether this reduction of current corresponded to inactivation of I_{to} and/or I_{Kur}, by applying the same steady-state inactivation protocol in the presence of 100 μM 4-AP (Fig. 8*B*), a concentration that does not block I_{to} (cf. Fig. 2). Our rationale was that if the reduction of current after positive prepulses corresponded to inactivation of I_{to}, we would observe a difference between the test pulse currents obtained with the −20, −30 and −40 mV inactivating prepulses. This was not the case; in the presence of 4-AP, the test pulse currents obtained with prepulses at −20, −30 and −40 mV superimposed (Fig. 8*B*) and did not show any inactivating component. This finding ensures that in this voltage range, the prepulse can completely inactivate I_{to}. These results also confirm that the choice of −40 mV as the prepulse voltage used to separate I_{to} and

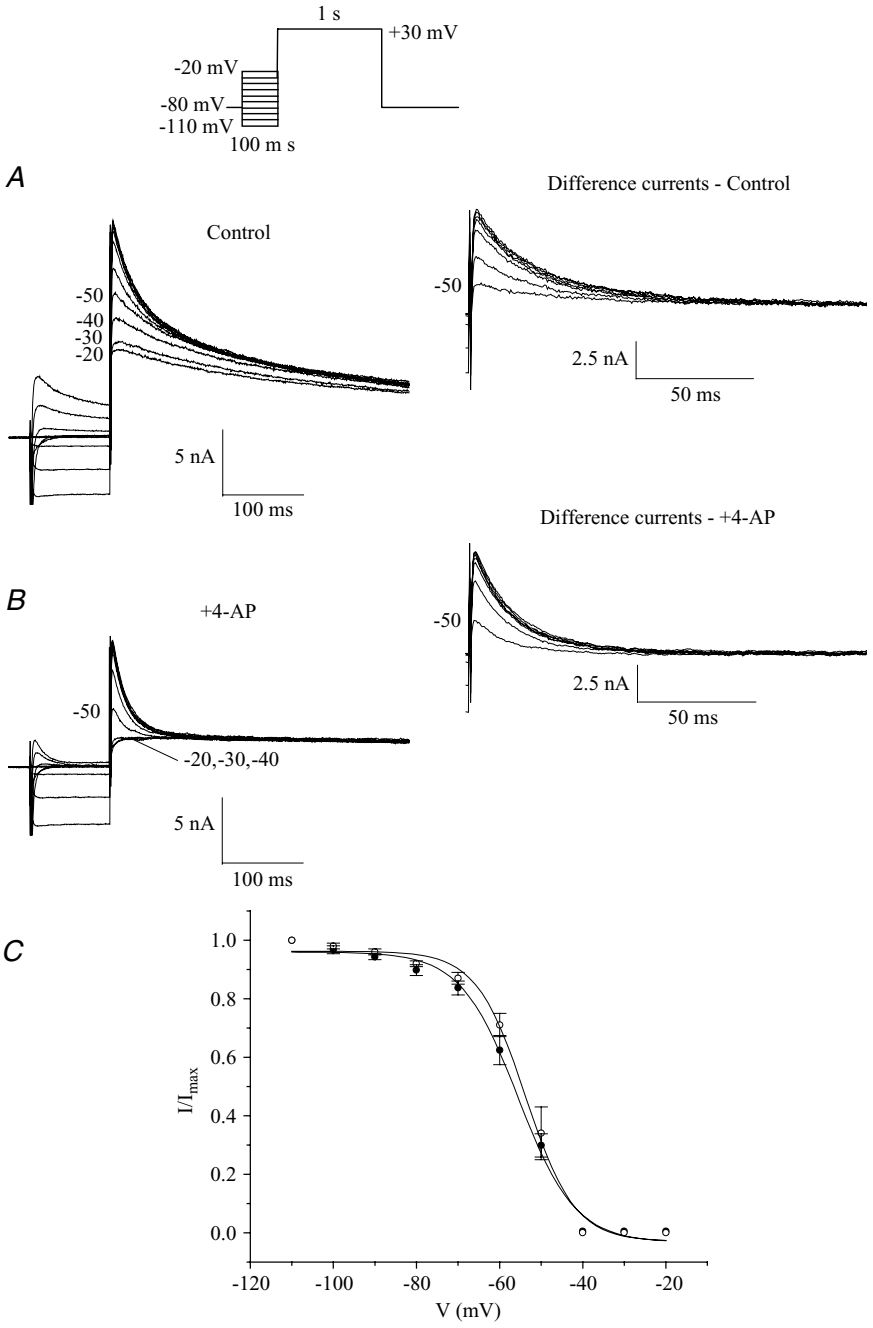

Figure 8. Voltage dependence of steady-state inactivation of I_{to} at room temperature (22°C)
A, example of a family of currents produced by a two-pulse voltage-clamp protocol. The 100 ms inactivating prepulse potential was varied from −110 to −20 mV; the test pulse potential was +30 mV (protocol shown at top). Numbers next to current records indicate corresponding potential of inactivating pulse. Inset in *A* shows difference currents: subtraction of the test pulse current following each prepulse from that obtained with the −40 mV prepulse. *B*, example of currents produced by the protocol used in *A* after superfusion of the same cell with 100 μM of 4-AP which eliminated I_{Kur} without affecting I_{to}. Inset in *B* shows difference currents: subtraction of the test pulse current following each prepulse from that obtained with the −40 mV prepulse. *C*, plot of voltage dependence of steady-state inactivation of I_{to} under control conditions (●) and in the presence of 4-AP (○). The amplitude of I_{to} for each prepulse membrane potential was determined by subtracting each test pulse current with that obtained with the −40 mV prepulse. The I_{to} test pulse amplitude was normalized to the amplitude at the most negative prepulse potential. Data points are mean ± S.E.M. (control, $n = 6$; +4-AP, $n = 4$). The smooth curves are the best-fit Boltzmann function (see Methods).

I_{Kur} is optimal. Indeed, choosing a more positive prepulse voltage (−30 mV) would inactivate a small portion of I_{Kur}, while choosing a more negative voltage (−50 mV) would not fully inactivate I_{to}.

Figure 8*C* presents mean data for steady-state inactivation of I_{to} under control conditions and in the presence of 100 μM 4-AP. The amplitude of I_{to} for each prepulse potential was determined by subtracting each test pulse current from that obtained with the 100 ms prepulse at −40 mV (data presented in insets on Fig. 8*A* and *B*). The normalized current data were fitted to a Boltzmann function (see Methods), yielding a half-inactivation potential of -55.8 ± 1.3 mV, and a mid-point slope factor of 6.6 ± 0.5 mV for I_{to} under control conditions, and -53.5 ± 1.9 mV and 5.5 ± 0.5 mV in the presence of 4-AP. Neither the respective half-inactivation potentials nor the mid-point slope factors were significantly different. In addition, Fig. 8*C* shows that inactivation of I_{to} is almost completely removed at the normal resting membrane potential of mouse ventricular cells, suggesting that this current plays an important functional role.

When the membrane potential dependence of steady-state inactivation of I_{to} was studied at 32°C very similar parameters were obtained (Fig. 9). At 32°C, the amplitude of I_{to} corresponding to each prepulse potential was determined by subtracting the test pulse current from that obtained with a 50 ms prepulse at −40 mV (see Fig. 4 for justification of the prepulse duration and data presented in insets on Fig. 9*A* and *B*). This protocol also yielded important information about the choice of the inactivating prepulse (50 ms at −40 mV) used to eliminate I_{to} at 32°C. Similar to the pattern of results obtained at room temperature, Fig. 9*A* shows that there was a progressive reduction of peak current when the inactivating voltage steps were varied from −40 to −20 mV. This reduction in current magnitude appeared to be associated with a decrease in the slow phase of inactivation of the current. We verified whether this reduction of current was due to reduction of I_{to}, I_{Kur} or both currents by repeating this protocol in the same myocyte in the presence of 100 μM 4-AP (i.e. in the absence of I_{Kur}). Figure 9*B* shows that the reduction of current observed in Fig. 9*A* was due to partial inactivation of I_{Kur} since the currents recorded following the −20, −30 and −40 mV inactivating pulses are superimposed in the presence of 4-AP. These results confirmed that at 32°C, a 50 ms inactivating prepulse at −40 mV was sufficient to completely inactivate I_{to}, with minimal effect on I_{Kur}. Very similar results were obtained on each of the six different cells studied.

Figure 9*C* presents mean data for steady-state inactivation of I_{to} under control conditions and in the presence of 100 μM 4-AP. The normalized current data were fitted to a Boltzmann function (see Methods), yielding a half-inactivation potential of -52.0 ± 0.7 mV, and a mid-point slope factor of 5.5 ± 0.6 mV for I_{to} under control conditions, and -51.4 ± 0.9 mV and 5.0 ± 0.5 mV in the presence of 4-AP. Neither the respective half-inactivation potentials nor the mid-point slope factors were significantly different. Similar to what was observed at 22°C, inactivation of I_{to} is almost completely removed at the normal resting membrane potential of mouse ventricular cells (Fig. 9*C*).

Data describing the kinetics of reactivation or recovery of I_{to} from inactivation are summarized in Fig. 10. The time course of recovery was measured using a two-pulse voltage-clamp protocol (see Methods). An example of a family of currents that illustrates the time course of recovery at −80 mV is shown in Fig. 10*A*. The membrane potential between the two pulses was changed to measure the time course of recovery at three different membrane potentials in the diastolic range. I_{to} amplitude was measured as the difference between peak current and current 150 ms after the peak, which corresponds to approximately 5 times its macroscopic inactivation time constant at +30 mV and 22°C (28.0 ± 1.2 ms, $n = 12$). The data of Fig. 10*B*, summarized from seven different myocytes, shows the time course of recovery at −60, −70 and −80 mV. Recovery was more rapid at more hyperpolarized potentials, and at −80 mV, near the normal resting membrane potential, recovery was complete in less than 200 ms. The mean data for each membrane potential were determined to approximate to single exponential functions (Fig. 10*B*), with time constants of 34.6 ms at −80 mV, 55.0 ms at −70 mV, and 117.8 ms at −60 mV. These recovery experiments were repeated at 32°C. I_{to} amplitude was measured as the difference between peak outward current and current 50 ms after the peak, which corresponds to approximately 5 times its macroscopic inactivation time constant at +30 mV and 32°C (9.9 ± 0.6 ms, $n = 10$). As expected, recovery from inactivation was faster at more physiological temperatures (at −80 mV, $\tau = 18.0 \pm 5.7$ ms, $n = 6$).

Inactivation/reactivation of I_{Kur} in adult mouse ventricular myocytes

The voltage dependence of steady-state inactivation of I_{Kur} was measured with a two-pulse protocol similar to that used for I_{to} (Fig. 8), except that the pulse durations were considerably longer because of the very much slower inactivation kinetics of I_{Kur}. Figure 11*A* shows an example of the membrane potential dependence of steady-state inactivation of I_{Kur} measured with a two-pulse protocol. Note that the preconditioning pulse of 5 s in duration (i.e. 50 times longer than the duration of the I_{to} inactivating prepulse) ensured that I_{Kur} was completely inactivated (cf. Fig. 3). A 100 ms pulse to −40 mV was interposed between the inactivating and test pulses; this

removed I_{to} from the test pulse current. Inactivating pulse potentials for the data shown in Fig. 11*A* ranged from −80 to −20 mV. Figure 11*B* summarizes normalized data from seven different myocytes. The Boltzmann function fitted to the data yielded a half-inactivation potential of -44.7 ± 1.7 mV, and a mid-point slope factor of 6.0 ± 0.6 mV. Steady-state inactivation was also studied at 32°C. The protocol included a 50 ms prepulse to −40 mV, as opposed to the 100 ms prepulse used at room temperature (see Fig. 4 for justification of the prepulse duration). At 32°C, the Boltzmann function fitted to the data yielded a half-inactivation potential of -48.3 ± 1.3 mV and mid-point slope factor of 5.8 ± 0.5 mV ($n = 12$).

Figure 11*C* describes the time course of recovery from inactivation of I_{Kur} at room temperature. The paired-pulse

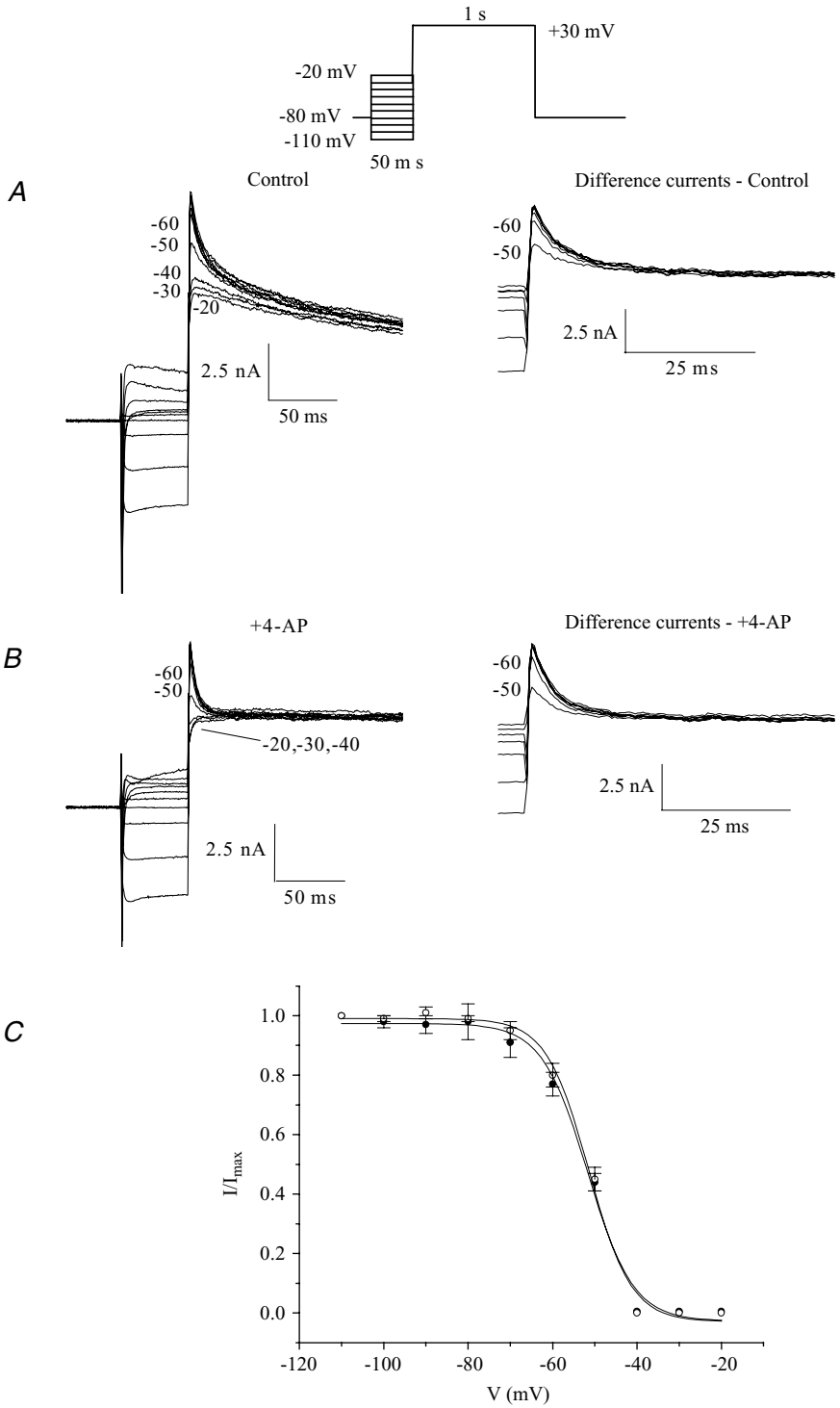

Figure 9. Voltage dependence of steady-state inactivation of I_{to} at 32°C
A, example of a family of currents produced by a two-pulse voltage-clamp protocol. A 50 ms inactivating prepulse potential was varied from −110 to −20 mV; the test pulse potential was +30 mV (protocol shown at top). Numbers next to current records indicate corresponding potential of inactivating pulse. Inset in *A* shows difference currents: subtraction of the test pulse current following each prepulse from that obtained with the −40 mV prepulse. *B*, example of currents produced by the protocol used in *A* after superfusion of the same cell with 100 μM of 4-AP which eliminated I_{Kur} without affecting I_{to}. Inset in *B* shows difference currents: subtraction of the test pulse current following each prepulse from that obtained with the −40 mV prepulse. *C*, plot of voltage dependence of steady-state inactivation of I_{to} under control conditions (●) and in the presence of 4-AP (○). The amplitude of I_{to} for each prepulse membrane potential was determined by subtracting each test pulse current from that obtained with the −40 mV prepulse. The I_{to} test pulse amplitude was normalized to the amplitude at the most negative prepulse potential. Data points are mean ± S.E.M. (control, $n = 6$; +4-AP, $n = 6$). The smooth curves are the best-fit Boltzmann function (see Methods).

protocol used to measure the time course of recovery was similar to that applied in I_{to} experiments, except that the inactivating pulse was 3-fold longer and both pulses were preceded by the I_{to} inactivating prepulse (100 ms, −40 mV). The current records shown in Fig. 11*C* demonstrate that I_{Kur} recovered from inactivation much more slowly than I_{to}. Recovery was measured at membrane potentials of −60, −70 and −80 mV, and data pooled from seven different myocytes are plotted in Fig. 11*D*. As for I_{to}, recovery of I_{Kur} from inactivation was more rapid for more hyperpolarized potentials, but the time constants for recovery of I_{Kur} were more than 20-fold greater than the corresponding time constants for recovery of I_{to}. When these experiments were repeated at 32°C, the reactivation time of I_{Kur} was found to be much faster than at room temperature (at −80 mV, $\tau = 441 \pm 45$ ms, $n = 13$). For these recovery experiments carried out at 32°C, the −40 mV prepulse duration was reduced to 50 ms.

Comparison of K^+ currents between adult mouse ventricular and atrial myocytes

To demonstrate that these voltage-clamp protocols, which we developed for studying K^+ current in mouse ventricle, can also be used to separate time- and voltage-dependent K^+ currents in other cell types, we applied the same voltage-clamp protocols to adult mouse atrial myocytes. The data presented in Fig. 12 compare the K^+ currents in adult mouse right ventricular and atrial myocytes recorded at room temperature. These findings show that the atrial K^+ currents consist of very similar components as those in adult mouse ventricular myocytes. The upper panel illustrates total K^+ current elicited by 500 ms voltage-clamp step to +30 mV, from a holding potential of −80 mV. As noted, in atrial cells, this depolarizing voltage step elicited outward current(s) with similar time and voltage dependence to those observed in ventricular myocytes. However, K^+ current density in atrial cells was 2- to 3-fold smaller. The current traces in the middle and lower panels of this figure compare K^+ currents recorded in the presence of the inactivating prepulse without (middle) or with 4-AP (lower). In summary, in atrial myocytes, a transient K^+ current (I_{to}) is inactivated by the prepulse, and low concentrations of 4-AP completely blocks a slowly inactivating current (I_{Kur}). A 4-AP-resistant component of outward K^+ current that does not display inactivation (I_{ss}) is also observed (Lomax *et al.* 2003). Figure 12*C* compares current densities (at +30 mV) for the three outward K^+ currents expressed in adult mouse right ventricular and atrial

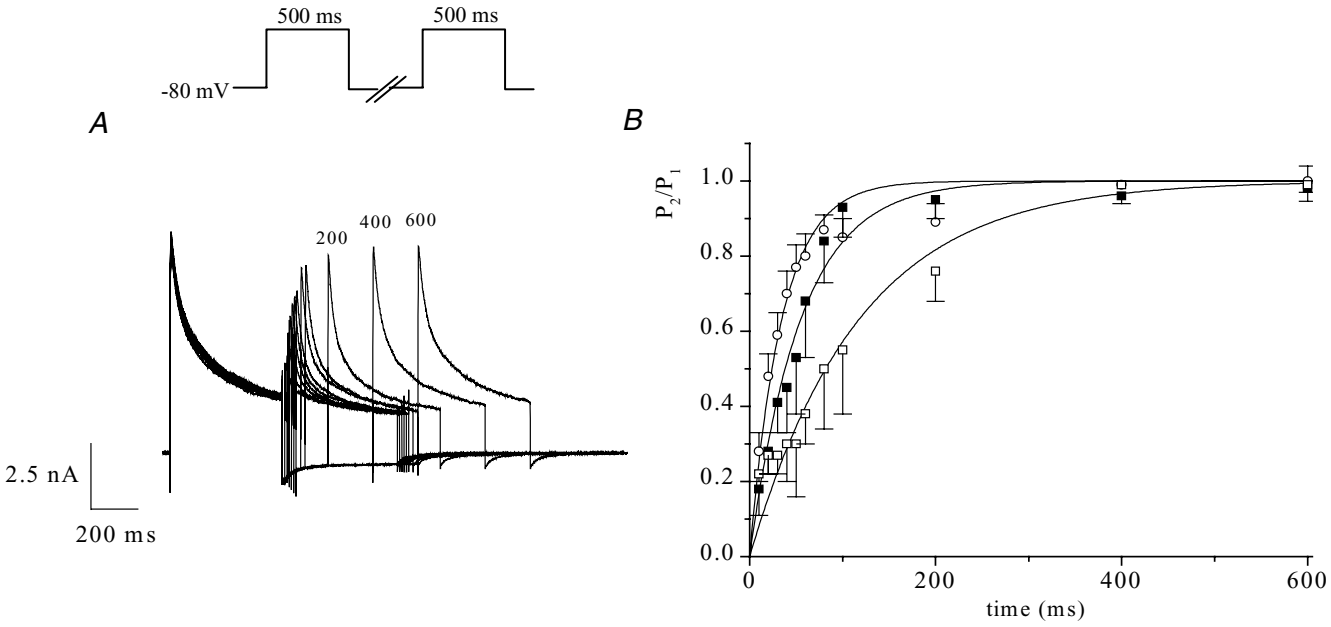

Figure 10. Time course of recovery of I_{to} from inactivation at room temperature (22°C)
A, example of a family of membrane currents produced by a two-pulse voltage-clamp protocol, showing the time course of recovery of I_{to} from inactivation. A 500 ms inactivating pulse (+ 30 mV) was followed at intervals of 10, 20, 30, 40, 50, 60, 80, 100, 200, 400 and 600 ms by an identical test pulse; numbers next to selected records indicate interpulse interval (ms). *B*, membrane potential dependence of recovery from inactivation of I_{to}. Data (mean ± S.E.M.) were pooled from 7 different cells. P_2/P_1 is the ratio of test pulse current/prepulse current amplitudes. I_{to} amplitude was measured as the difference between peak outward current and current 150 ms after the peak. Recovery was measured at interpulse potentials of −60 mV (□), −70 mV (■) and −80 mV (○). The smooth lines are best-fit single exponential functions with time constants of 35 ± 2 ms for −80 mV, 55 ± 3 ms for −70 mV and 118 ± 9 ms for −60 mV.

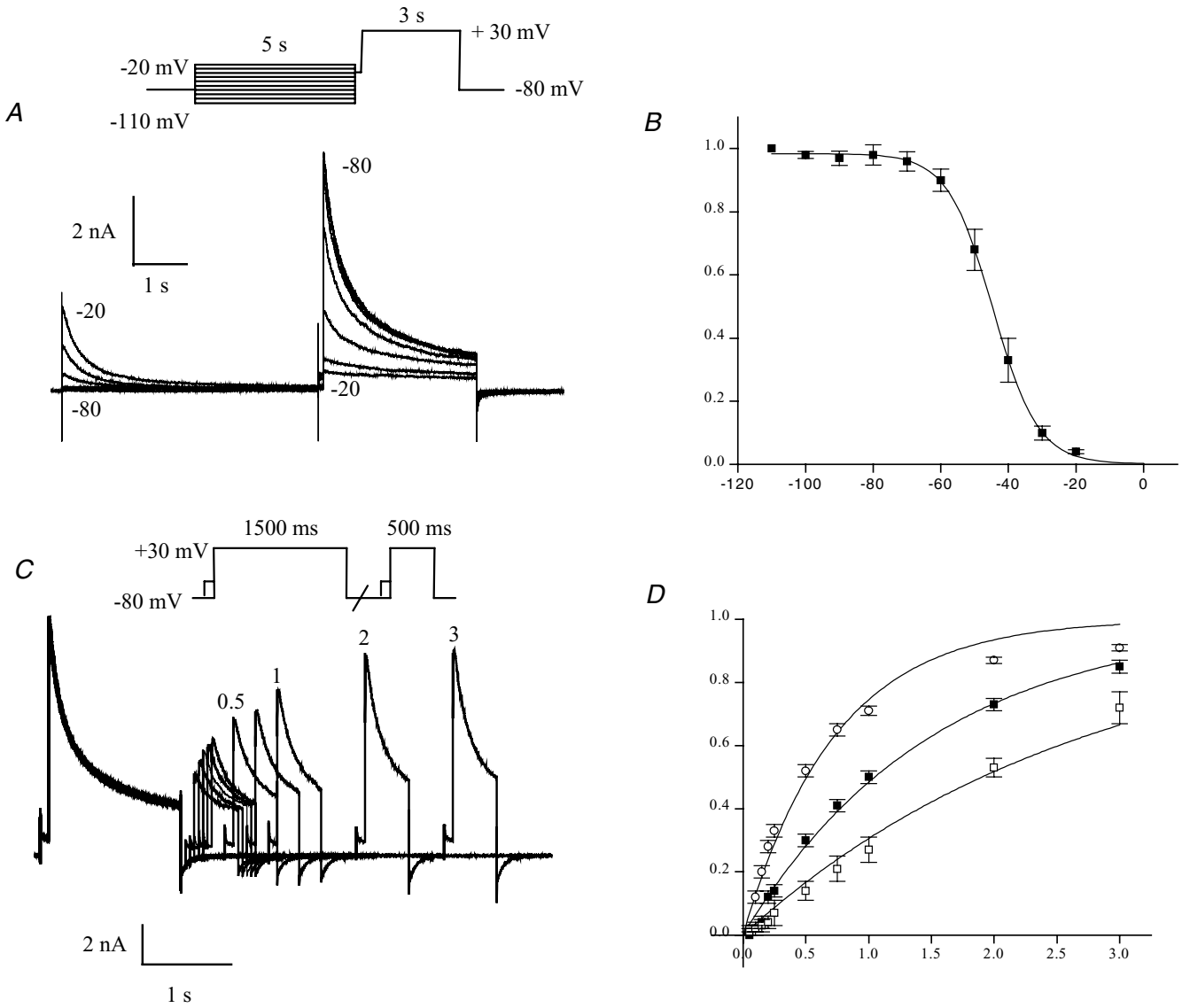

Figure 11. Inactivation of I_{Kur} at room temperature (22°C)
A and *B*, membrane potential dependence of steady-state inactivation of I_{Kur}. *A*, example of a family of currents produced by a two-pulse voltage-clamp protocol. Inactivating pulse (5 s duration) was varied from −110 to −20 mV; the test pulse potential was +30 mV. Numbers next to current records indicate membrane potential for the corresponding inactivating pulse. Traces obtained with inactivation pulse ranging from −80 to −20 mV are shown. *B*, plot of voltage dependence of steady-state inactivation of I_{Kur}. The I_{Kur} test pulse amplitude was normalized to the test amplitude for the most negative prepulse potential. I_{Kur} was obtained by subtraction of the current at the end of the test pulse from the peak test pulse current. Data were pooled from 7 different myocytes. Data points are mean ± S.E.M. The smooth curve is the best-fit Boltzmann function (see Methods). *C* and *D*, time course of recovery of I_{Kur} from inactivation. *C*, example of a family of membrane currents produced by a two-pulse voltage-clamp protocol, showing the time course of recovery from inactivation of I_{Kur}. A 1.5 s inactivating pulse was followed at intervals between 50 ms and 3 s by a 500 ms test pulse. Both inactivating and test pulses were preceded by a brief (100 ms at −40 mV) pulses to inactivate I_{to}. The holding and interpulse potentials were −80 mV. Numbers next to selected records indicate interpulse interval, in seconds. *D*, membrane potential dependence of recovery from inactivation of I_{Kur}. Data (mean ± S.E.M.) were pooled from 7 different cells. P_2/P_1 is the ratio of test pulse current/inactivating pulse current amplitudes. I_{Kur} amplitude was measured by the difference between peak inactivating or test pulse current and the current at the end of the inactivating pulse. Recovery was measured at interpulse potentials of −60 mV (□), −70 mV (■) and −80 mV (○). The smooth lines are best-fit single exponential functions with time constants of 0.74 ± 0.04 s for −80 mV, 1.51 ± 0.06 s for −70 mV and 2.74 ± 0.13 s for −60 mV.

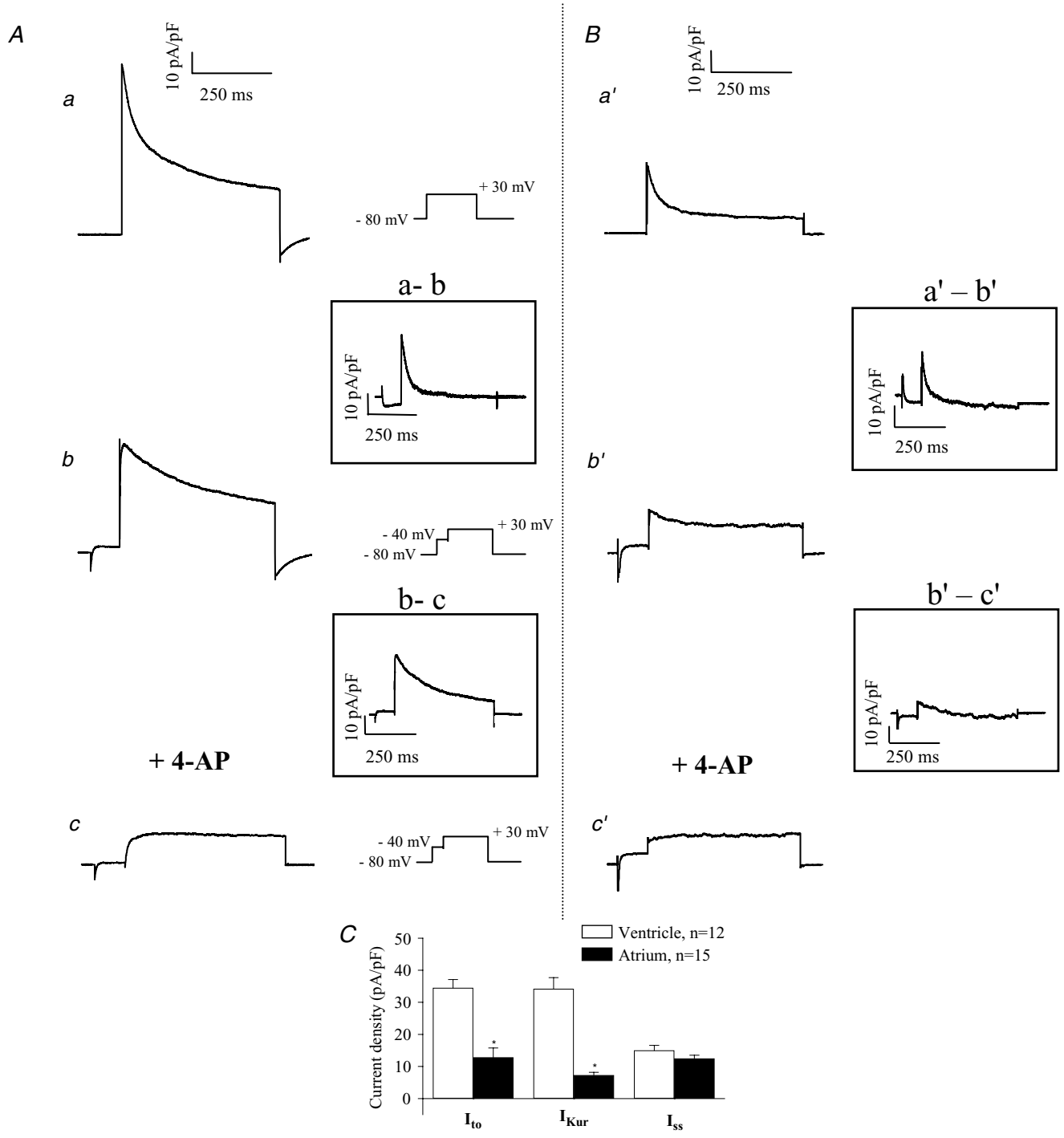

Figure 12. Comparison of the K^+ currents in adult mouse ventricular (*A*) and atrial (*B*) myocytes at room temperature

Upper records, current traces produced by 500 ms steps to +30 mV (HP −80 mV). Middle records, current traces produced by a 500 ms step to +30 mV preceded by an inactivating prepulse (100 ms, −40 mV). The potential-sensitive 'difference' currents (I_{to}) obtained by digital subtraction of currents recorded with and without inactivating prepulse, are shown in the inset. Lower records, current records obtained in the presence of both the inactivating prepulse and 4-AP. The 4-AP-sensitive 'difference' currents, obtained by digital subtraction, are shown in the inset. *C*, bar graph comparing the current density of I_{to}, I_{Kur} and I_{ss} in adult mouse ventricular and atrial myocytes. The test potential was +30 mV from an HP of −80 mV. Data (mean ± S.E.M.) was averaged from 12 different ventricular and 15 atrial myocytes.

myocytes. These plots show that in atrial myocytes the current densities of I_{to} and I_{Kur} are significantly smaller than in adult mouse ventricle. Compared to the large I_{Kur} in ventricular myocytes (34.2 ± 3.5 pA pF^{-1}), I_{Kur} in adult atrial cells was smaller (7.3 ± 0.9 pA pF^{-1}). Also, the density of I_{to} measured at +30 mV was much larger in the ventricle compared to the atrium (34.5 ± 2.6 and 12.8 ± 2.9 pA pF^{-1}, respectively). Finally, we found that the electrophysiological features as well as the current density of I_{ss} were very similar between mouse ventricle and atrium (I_{ss} at +30 mV, 15.6 ± 1.6 and 12.6 ± 1.6 pA pF^{-1}, respectively).

Comparison of expression of K^+ channel isoforms in adult mouse ventricle and atrium

RNase protection assays were used to compare the RNA levels of Kv1.5 (encoding I_{Kur}), Kv2.1 (underlying I_{ss}), Kv4.2 and Kv4.3 (responsible for I_{to}) in adult mouse ventricular and atrial tissue. Figure 13*A* consists of an autoradiogram showing the relative levels of Kv1.5 transcript in adult mouse ventricle and atrium. This K^+ channel α-subunit is expressed in both tissues; however, Kv1.5 is expressed at a much higher level in ventricle than in atrium. Quantification of mRNA levels (see Methods) showed that Kv1.5 transcripts were more than 3-fold more abundant in ventricle than in atrium. Kv2.1, Kv4.2 and Kv4.3 transcripts were also detected in both atrium and ventricle (Fig. 13*B* and *C*). Kv2.1 and Kv4.3 were detected at similar levels in both tissues, while the expression of Kv4.2 was higher in the ventricle.

Discussion

Summary of findings

Our results demonstrate the utility of a biophysical and pharmacological approach for separating the three main time- and voltage-dependent components of K^+ current which are expressed in cardiac myocytes isolated from the hearts of adult mice. This approach provides an accurate description of densities and kinetic properties of these K^+ conductances during the time course of an action potential. In addition, information regarding their functional significance in action potential repolarization is made available during each experiment. In agreement with previous analyses (Fiset *et al.* 1997*a*; Trépanier-Boulay *et al.* 2001; Brouillette *et al.* 2003), our results show that the time- and voltage-dependent K^+ currents in adult mouse ventricular myocytes can be separated using protocols that take advantage of their distinct kinetics and dependence on membrane potential, as well as differential sensitivity to the K^+ channel blocker, 4-AP. In the present study, data were obtained at both 22 and 32°C. As expected from classical findings and theory, our results confirm that this approach for separation of these components of K^+ current is as effective at 'physiological' temperatures as it is at room temperature, although the duration of the inactivating prepulse has to be adapted to the altered current kinetics at 32°C.

I_{Kur} is a rapidly activating but slowly inactivating outward current, which apart from its very much slower rates of inactivation, clearly differs from I_{to} by its much higher sensitivity to 4-AP. The IC_{50} of 4-AP for I_{to} is ~10-fold higher than that of I_{Kur} (Wettwer *et al.* 1993; Campbell *et al.* 1995; Fiset *et al.* 1997*a*). As a consequence, by applying an inactivating prepulse and by using a low concentration of 4-AP, we have been able to separate I_{Kur} and I_{to}. A third component of outward K^+ current is much more slowly activating, and shows virtually no inactivation, even for depolarizations lasting several seconds. This component, I_{ss}, can be distinguished from I_{Kur} on the basis of its sensitivity to 4-AP; I_{ss} is not affected by concentrations of 4-AP that completely block I_{Kur} (Zhou *et al.* 1998; Xu *et al.* 1999*b*). Our data show that this K^+ current is distinctly different from either I_{to} or I_{Kur}, and provide evidence that its slow activation kinetics are not an experimental artefact due to complex channel blocking actions of 4-AP.

Previous work has provided strong evidence for the general pattern of K^+ current expression which we have determined in adult mouse ventricle (e.g. Xu *et al.* 1999*b*; Nerbonne, 2000). The majority of these studies have made use of knockout or dominant negative strategies to eliminate targeted K^+ channel α-subunits. The resulting changes in action potential waveform have been convincingly related to the documented alterations in K^+ currents using off-line biophysical analysis based on curve fits of a mathematical expression consisting of sums of exponential functions to the experimental data. Our approach differs fundamentally and, as illustrated, can be used to advantage during an experiment, without concerns about cellular/tissue adaptations to genetic manipulations. Our data (Figs 5, 6 and 7) in conjunction with previously published findings provide important insights into the functional roles of I_{to}, I_{Kur} and I_{ss}.

Recent papers from our group illustrate how the experimental approach described here can also be used to separate the K^+ currents which are expressed in adult mouse atrium (Lomax *et al.* 2003) and in adult mouse ventricular endocardial myocytes (Kuo *et al.* 2001) where $I_{to,s}$ (Kv1.4) (Guo *et al.* 1999) is present.

Action potential repolarization

With this experimental design and our approach for data analysis, it is possible to determine the relative magnitudes of the three outward components, and hence to deduce their relative contributions to the peak *I–V* relationship and action potential repolarization. As mentioned, in

right ventricular myocytes, the peak current densities of I_{Kur} and I_{to} were not significantly different, while I_{ss} was significantly smaller than either I_{Kur} or I_{to} (Fig. 5). These findings and the clear differences in activation and inactivation rates amongst these three K^+ currents reveal their roles in repolarization of the action potential. The large magnitude and rapid activation kinetics of both I_{to} and I_{Kur} result in these currents making a major contribution to early repolarization of action potential. In contrast, the activation of I_{ss} is more than 10-fold slower than either I_{to} or I_{Kur} at a membrane potential of +10 mV. Consequently, this K^+ current would be expected to make a much smaller contribution to the total peak outward current. In keeping with this, Zhou *et al.* (1998) reported that high concentrations of tetraethylamonium (TEA; which block I_{ss}) produced only a slight inhibition of the outward current in mouse ventricular myocytes. In their study, the amplitude of the TEA-sensitive current was < 10% of total outward current. In addition, inhibition of this current by TEA did not significantly alter action potential duration, suggesting that the TEA-sensitive current does not play a major role in determining the action potential waveform. This finding is consistent with another study of Zhou *et al.* (2003) which showed only a small effect of 5 mM TEA on the APD of mouse ventricle. However, DuBell *et al.* (2000) have reported that 20 mM TEA produced a marked prolongation of APD. In the present study, we have examined the possibility that this discrepancy in the contribution of a TEA-sensitive component to the action potential may be related to the difference in recording temperatures between the study of duBell *et al.* (32°C) and those of the other groups which were carried out at room temperature. To do so, we evaluated the contribution of the TEA-sensitive current on the action potential duration at room temperature and at 32°C. We observed that 20 mM TEA produces a similar prolongation of APD_{90} at 22 and 32°C (26 ± 9 and 39 ± 4%, respectively, $n = 3$, $P = 0.2$). However, based on these data and the known non-linear relationship between K^+ current magnitude and rate of repolarization of the action potential, it is not possible to define the contribution of I_{ss} to the APD. In fact, our TEA experiments showed that, in addition to block of most of I_{ss}, 20 mM TEA also inhibited a small portion of both I_{Kur} and the inwardly rectifying background K^+ current, I_{K1}.

As shown in Fig. 5, I_{to}, I_{Kur} and I_{ss} inactivate at very different rates; I_{Kur} inactivated 10- to -20-fold more slowly than I_{to}, while I_{ss} inactivates very little, even during a depolarization of 5 s duration. In addition and more importantly for physiological responses, the time course of reactivation of I_{to} was much faster than that of I_{Kur} at diastolic membrane potentials. Note that the time constants for recovery from inactivation of I_{Kur} were more than 20-fold greater than the corresponding time constants for I_{to} at membrane potentials in the normal diastolic range. These findings have important implications for the relative role of these K^+ currents at (i) the very high heart rate of the mouse and (ii) when heart rate is changed in response to physiological or imposed stimuli.

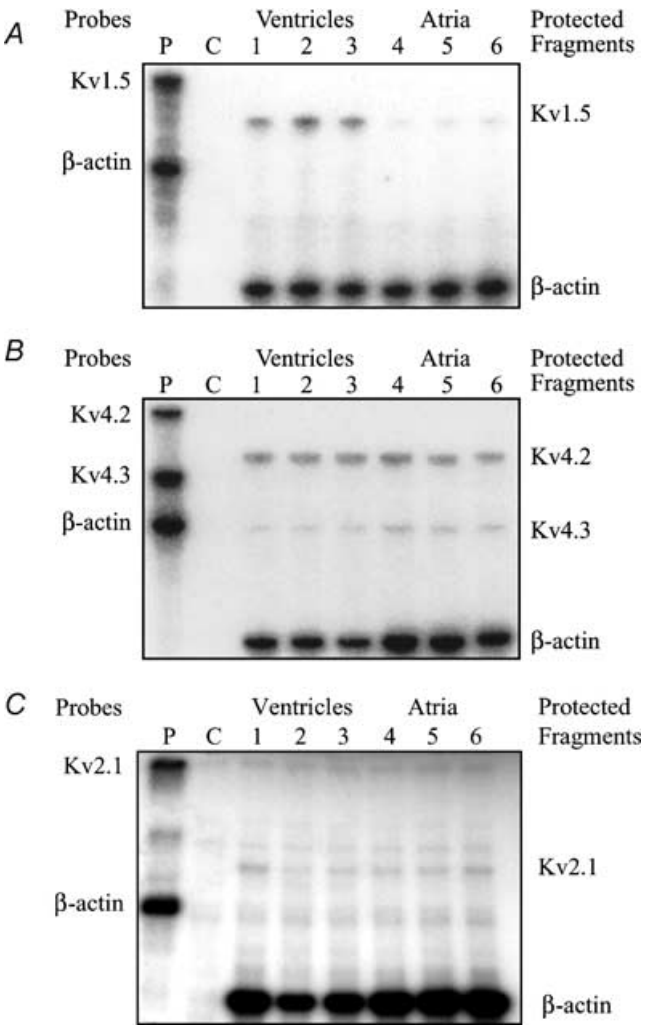

Figure 13. Comparison of K^+ channel mRNA expression between adult mouse ventricle and atrium
RNase protection assays depicting K^+ channel expression to compare adult mouse atrium and ventricle. Panels show autoradiographs of polyacrylamide gels. Radioactively labelled antisense riboprobes specific for mouse K^+ channel isoforms were hybridized with total RNA (2.5 μg) from atrium or ventricle and digested with RNaseA/T1. Reaction mixtures were analysed by polyacrylamide gel electrophoresis, followed by autoradiography. See Methods section for details. *A*, comparison of Kvl.5 RNA expression in atrium and ventricle. Lane P shows undigested riboprobes for Kvl.5 and for β-actin (which was used as the internal control). Lane C is yeast RNA, which is the negative control. Post-digest (protected fragments) for Kvl.5 and β-actin were run simultaneously in three lanes each for atrial and ventricular RNA samples. Note that the β-actin signal was very similar in all six lanes. *B*, comparison of Kv4.2 and Kv4.3 RNA expression levels in atrium and ventricle. *C*, comparison of Kv2.1 RNA expression levels in atrium and ventricle.

Comparisons of the expression of different K^+ currents/channels in adult mouse ventricle and atrium

Electrophysiological data obtained with the approach described here show that all the major K^+ currents expressed in adult mouse ventricular myocytes are also expressed in adult mouse atrial myocytes (Lomax *et al.* 2003). In keeping with this, our studies of the levels of expression showed that all the K^+ channel isoforms examined (Kv1.5, Kv2.1, Kv4.2 and Kv4.3) are present in both mouse ventricular and atrial tissues. The largest difference in K^+ channel expression between atrium and ventricle was for the Kv1.5 transcript: it was more than 3-fold more abundant in ventricle than in atrium. These expression data are consistent with the electrophysiological results obtained in both ventricle and atrium. In adult mouse heart, I_{Kur} shows significant chamber-specific expression. Although this current is relatively small in mouse atrial myocytes, it is a large and hence important repolarizing current in ventricle. All electrophysiological properties of I_{to} were very similar between atrium and ventricle; however, the density of this current was much larger in the ventricle compared to the atrium (Fig. 12) (Lomax *et al.* 2003). The mRNA experiments showed that Kv4.2 and Kv4.3 were both expressed at significant levels in mouse atrium and ventricle. Kv4.2 was expressed at about 80% higher levels in ventricle compared with atrium, while Kv4.3 was expressed at approximately equal levels in both tissues. These findings suggest that the chamber-specific difference in the expression of I_{to} may be related to Kv4.2 expression. The density of I_{ss} as well as Kv2.1 mRNA expression were similar between atrium and ventricle.

Contribution of K^+ channel β-subunits

Voltage-gated K^+ channels are protein complexes composed of four integral membrane α-subunits and up to four cytoplasmic β-subunits (England *et al.* 1995*a*; Bekeler-Arcuri *et al.* 1996). β-Subunit association can contribute to the diversity of K^+ currents in mammalian myocardium (England *et al.* 1995*b*). β-Subunits associate with the channel-forming α-subunits of K^+ channels, influencing both the kinetics of these channels and their targeting/insertion into the plasmalemma (Li *et al.* 1992; Rettig *et al.* 1994; Majumder *et al.* 1995; England *et al.* 1995*a*,*b*; Shi *et al.* 1996; Fink *et al.* 1996; Uebele *et al.* 1996, 1998). These distinct forms of regulatory interactions among the principal and β-subunits of the voltage-gated K^+ channels serve to increase greatly the flexibility of their regulation and may play a critical role in defining the physiological properties of excitable cells (Isom *et al.* 1994). Detailed examination of the functional role(s) of the β-subunits was not addressed in the present study, since we recognized that each subunit requires a complete electrophysiological/biophysical study. We note, however, that the approach for rapid, semiquantitative determination of K^+ current size and time course made possible by the methods developed and validated in this study will be essential for meaningful assessment of modulation of mouse heart repolarization by β-subunits, experimental pharmacological agents, autonomic transmitters or cotransmitters.

In summary, our action potential recordings, in combination with voltage-clamp data, strongly suggest that in ventricular myocytes, early repolarization is brought about by activation of both I_{to} and I_{Kur}. In the final phase of repolarization, I_{Kur}, I_{K1} and possibly I_{ss} contribute to outward current (Figs 5, 6 and 7). These results, in combination with the recovery or reactivation data (Figs 10 and 11) and steady-state inactivation curves (Figs 8 and 11), provide significant new insights into several important aspects of the electrophysiology of the mouse heart.

References

Agus ZS, Dukes ID & Morad M (1991). Divalent cations modulate the transient outward current in rat ventricular myocytes. *Am J Physiol* **261**, C310–C318.

Babij P, Askew R, Nieuwenhuijsen B, Su CM, Bridal TR, Jow B, Argentieri TM, Kulik J, DeGennaro LJ, Spinelli W & Colatsky TJ (1998). Inhibition of cardiac delayed rectifier K^+ current by overexpression of the Long-QT syndrome HERG G628S mutation in transgenic mice. *Circ Res* **83**, 668–678.

Barry DM, Xu H, Schuessler RB & Nerbonne JM (1998). Functional knockout of the transient outward current, long-QT syndrome, and cardiac remodelling in mice expressing a dominant-negative Kv4 α-subunit. *Circ Res* **83**, 560–567.

Bekeler-Arcuri X, Matos MF, Manganas L, Strassle BW, Monaghan MM, Rhodes KJ & Trimmer JS (1996). Generation and characterization of subtype-specific monoclonal antibodies to K^+ channel α- and β-subunit polypeptides. *Neuropharmacology* **35**, 851–865.

Benndorf K, Markwardt F & Nilius B (1987). Two types of transient outward currents in cardiac ventricular cells of mice. *Pflug Arch* **409**, 641–643.

Bondarenko VE, Szigeti GP, Bett GC, Kim S-J & Rasmusson RL (2004). A computer model of the action potential of mouse ventricular myocytes. *Am J Physiol Heart Circ Physiol* **287**, H1387–H1403.

Brouillette J, Trepanier-Boulay V & Fiset C (2003). Effect of androgen deficiency on mouse ventricular repolarization. *J Physiol* **546**, 403–413.

Brunet S, Aimond F, Li H, Guo W, Eldstrom J, Fedida D, Yamada KA & Nerbonne JM (2004). Heterogeneous expression of repolarizing, voltage-gated K^+ in adult mouse ventricles. *J Physiol* **559**, 103–120.

Campbell DL, Rasmusson RL, Comer MB & Strauss HC (1995). The cardiac calcium-independent transient outward potassium current: kinetics, molecular porperties, and role in ventricular repolarization. In *Cardiac Electrophysiology: from Cell to Bedside*, ed. Zipes DP & Jalife J, pp. 83–96. W.B. Saunders, Philadelphia, PA, USA.

Danik S, Cabo C, Chiello C, Kang S, Wit AL & Coromilas J (2002). Correlation of repolarization of ventricular monophasic action potential with ECG in the murine heart. *Am J Physiol* **283**, H372–H381.

Majumder K, De BM, Wang Z & Wible BA (1995). Molecular cloning and functional expression of a novel potassium channel beta-subunit from human atrium. *FEBS Lett* **361**, 13–16.

DuBell WH, Lederer WJ & Rogers TB (2000). K(+) currents responsible for repolarization in mouse ventricle and their modulation by FK-506 and rapamycin. *Am J Physiol* **278**, H886–H897.

England SK, Uebele VN, Kodali J, Bennett PB & Tamkun MM (1995*b*). A novel K^+ channel β subunit (hKvß1.3) is produced via alternative mRNA splicing. *J Biol Chem* **270**, 28531–28534.

England SK, Uebele VN, Shear H, Kodali J, Bennett PB & Tamkun MM (1995*a*). Characterization of a voltage-gated K^+ channel β subunit expressed in human heart. *Proc Natl Acad Sci* **92**, 6309–6313.

Fink M, Duprat F, Lesage F, Heurteaux C, Romey G, Barhanin J & Lazdunski M (1996). A new K^+ channel β subunit to specifically enhance Kv2.2 (CDRK) expression. *J Biol Chem* **271**, 26341–26348.

Fiset C, Clark RB, Larsen TS & Giles WR (1997*a*). A rapidly activating sustained K^+ current modulates repolarization and excitation-contraction coupling in adult mouse ventricle. *J Physiol* **504**, 557–563.

Fiset C, Clark RB, Shimoni Y & Giles WR (1997*b*). *Shal*-type channels contribute to the Ca^{2+}-independent transient outward K^+ current in rat ventricle. *J Physiol* **500**, 51–64.

Guo W, Li H, London B & Nerbonne JM (2000). Functional consequences of elimination of $I_{to,f}$ and $I_{to,s}$. Early afterdepolarizations, atrioventricular block, and ventricular arrhythmias in mice lacking Kv1.4 and expressing a dominant-negative Kv4 α subunit. *Circ Res* **87**, 73–79.

Guo W, Xu H, London B & Nerbonne JM (1999). Molecular basis of transient outward K^+ current diversity in mouse ventricular myocytes. *J Physiol* **521**, 587–599.

Heath BM, Xia J, Dong E, An RH, Brooks A, Liang C, Federoff HJ & Kass RS (1998). Overexpression of nerve growth factor in the heart alters ion channel activity and beta-adrenergic signalling in an adult transgenic mouse. *J Physiol* **512**, 779–791.

Isenberg G & Klockner U (1982). Calcium tolerant ventricular myocytes prepared by preincubation in a 'KB medium'. *Pflug Arch* **395**, 6–18.

Isom LL, De Jongh KS & Catterall WA (1994). Auxiliary subunits of voltage-gated ion channels. *Neuron* **12**, 1183–1194.

Jeron A, Mitchell GF, Zhou J, Murata M, London B, Buckett P, Wiviott SD & Koren G (2000). Inducible polymorphic ventricular tachyarrhythmias in a transgenic mouse model with a long QT phenotype. *Am J Physiol* **278**, H1891–H1898.

Josephson IR, Sanchez-Chapula J & Brown AM (1984). Early outward current in rat single ventricular cells. *Circ Res* **54**, 157–162.

Knollmann BC, Katchman AN & Franz MR (2001). Monophasic action potential recordings from intact mouse heart: validation, regional heterogeneity, and relation to refractoriness. *J Cardiovasc Electrophysiol* **12**, 1286–1294.

Knollmann BC, Knollmann-Ritschel BEC, Weissman NJ, Jones LR & Morad M (2000). Remodelling of ionic currents in hypertrophied and failing hearts of transgenic mice overexpressing calsequestrin. *J Physiol* **525**, 483–498.

Kuo HC, Cheng CF, Clark RB, Lin JJC, Lin JLC, Hoshijima M, Nguyen-Tran VTB, Gu Y, Ikeda Y, Chu PH, Ross J Jr, Giles WR & Chien KR (2001). A defect in the Kv channel-interacting protein 2 (KChIP2) gene leads to a complete loss of I_{to} and confers susceptibility to ventricular tachycardia. *Cell* **107**, 801–813.

Li M, Jan YN & Jan LY (1992). Specification of subunit assembly by the hydrophilic amino-terminal domain of the Shaker potassium channel. *Science* **257**, 1225–1230.

Lomax AE, Kondo CS & Giles WR (2003). Comparison of time- and voltage-dependent K^+ currents in myocytes from left and right atria of adult mice. *Am J Physiol* **285**, H1837–H1848.

London B, Guo W, Pan X, Lee JS, Shusterman V, Rocco CJ, Logothetis DA, Nerbonne JM & Hill JA (2001). Targeted replacement of Kv1.5 in the mouse leads to loss of the 4-aminopyridine-sensitive component of $I_{K,slow}$ and resistance to drug-induced QT prolongation. *Circ Res* **88**, 940–946.

London B, Jeron A, Zhou J, Buckett P, Han X, Mitchell GF & Koren G (1998*a*). Long QT and ventricular arrhythmias in transgenic mice expressing the N-terminus and first transmembrane segment of a voltage-gated potassium channel. *Proc Natl Acad Sci* **95**, 2926–2931.

London B, Wang DW, Hill JA & Bennett PB (1998*b*). The transient outward current in mice lacking the potassium channel gene Kv1.4. *J Physiol* **509**, 171–182.

Nerbonne JM (2000). Molecular basis of functional voltage-gated K^+ channel diversity in the mammalian myocardium. *J Physiol* **525**, 285–298.

Rettig J, Heinemann SH, Wunder F, Lorra C, Parcej DN, Dolly JO & Pongs O (1994). Inactivation properties of voltage-gated K^+ channels altered by presence of beta-subunit. *Nature* **26**, 289–294.

Shi G, Nakahira K, Hammond S, Rhodes KJ, Schechter LE & Trimmer JS (1996). β-Subunits promote K^+ channel surface expression through effects on early in biosynthesis. *Neuron* **16**, 843–852.

Trépanier-Boulay V, St-Michel C, Tremblay A & Fiset C (2001). Gender-based differences in cardiac repolarization in mouse ventricle. *Circ Res* **89**, 437–444.

Tseng GN, Jiang M & Yao JA (1996). Reverse use dependence of Kv4.2 blockade by 4-aminopyridine. *J Pharmacol Exp Ther* **279**, 865–876.

Uebele VN, England SK, Chaudhary A, Tamkun MM & Snyders DJ (1996). Functional differences in Kv1.5 currents expressed in mammalian cell lines are due to the presence of endogenous Kv beta 2.1 subunits. *J Biol Chem* **271**, 2406–2412.

Uebele VN, England SK, Gallagher DJ, Snyders DJ, Bennett PB & Tamkun MM (1998). Distinct domains of the voltage-gated K^+ channel Kv beta 1.3 beta-subunit affect voltage-dependent gating. *Am J Physiol* **274**, C1485–C1495.

Wang L & Duff HJ (1997). Developmental changes in transient outward current in mouse ventricle. *Circ Res* **81**, 120–127.

Wettwer E, Amos GJ, Gath J, Zerkowski HR, Reidemeister JC & Ravens U (1993). Transient outward current in human and rat ventricular myocytes. *Cardiovasc Res* **27**, 1662–1669.

Wickenden AD, Lee P, Sah R, Huang Q, Fishman GI & Backx PH (1999). Targeted expression of a dominant-negative Kv4.2 K^+ channel subunit in the mouse heart. *Circ Res* **85**, 1067–1076.

Xu H, Barry DM, Li H, Brunet S, Guo W & Nerbonne JM (1999*a*). Attenuation of the slow component of delayed rectification, action potential prolongation, and triggered activity in mice expressing a dominant-negative Kv2 α subunit. *Circ Res* **85**, 623–633.

Xu H, Guo W & Nerbonne JM (1999*b*). Four kinetically distinct depolarization-activated K^+ currents in adult mouse ventricular myocytes. *J General Physiol* **113**, 661–677.

Zaritsky JJ, Redell JB, Tempel BL & Schwarz TL (2001). The consequences of disrupting cardiac inwardly rectifying K^+ current (I_{K1}) as revealed by the targeted deletion of the murine Kir2.1 and Kir2.2 genes. *J Physiol* **533**, 697–710.

Zhou J, Jeron A, London B, Han X & Koren G (1998). Characterization of a slowly inactivating outward current in adult mouse ventricular myocytes. *Circ Res* **83**, 806–814.

Zhou J, Kodirov S, Murata M, Buckett PD, Nerbonne JM & Koren G (2003). Regional upregulation of Kv2.1-encoded current, $I_{K,slow2}$, in Kv1DN mice is abolished by crossbreeding with Kv2DN mice. *Am J Physiol* **284**, H491–H500.

Acknowledgements

This study was supported by operating and personnel grants from the Canadian Institutes of Health Research, the Heart and Stroke Foundation of Canada and Quebec, the Fonds de Recherche en Santé du Québec and the Foundation of the Montreal Heart Institute. J.B. has a CIHR Studentship Award. W.G. was supported by a Research Chair from the Heart and Stroke Foundation of Alberta and the Northwest Territories. The authors wish to thank V. Trépanier-Boulay, M.-A. Lupien, M. Marmabassi, K. Janzen and R. Winkfein for technical assistance.